Gender–dependent Influence of Endogenous Estrogen in Pulmonary Hypertension.

Kirsty M. Mair[1], Audrey F Wright[1], Nicholas Duggan[2], David J. Rowlands[2], Martin J. Hussey[2], Sonia Roberts[2], Josephine Fullerton[1], Margaret Nilsen[1], Lynn Loughlin[1], Matthew Thomas[2] & Margaret R. MacLean[1*].

[1]Institute of Cardiovascular and Medical Sciences, College of Medical and Veterinary Science, University of Glasgow, UK. [2] Novartis Institutes of BioMedical Research, Horsham, West Sussex, UK.

Corresponding Author: Margaret R MacLean PhD MBE FRSE, Institute of Cardiovascular and Medical Sciences, College of Medical, Veterinary and Life Sciences, University of Glasgow, UK. Phone: + 44 (0) 141 330 4768. Fax: +44 (0) 141 330 5481. Email: mandy.maclean@glasgow.ac.uk

Word Count: 3498.

Running title: Estrogen, gender and pulmonary hypertension. **Descriptor number:** 17.6

At a Glance Commentary: Females develop pulmonary arterial hypertension (PAH) more frequently that males. The role of estrogen in this female susceptibility is poorly understood. Our research shows that inhibition of endogenous estrogen synthesis using an aromatase inihibitor or inhibition of estrogen receptor alpha has therapeutic effects and restores BMPR2 expression in female but not male models of PAH. These findings suggest estrogen plays a pathogenic role in the pathology of PAH specifically in females

---

[*]**Author contributions:** Involvement in the conception, hypotheses delineation, and design of the study – KMM, ND, DJR, MJH, AFW, MT, MRM. Acquisition of the data or the analysis and interpretation of such information – KMM, ND, SR, JF, MN, AFW, MRM. Writing the article or substantial involvement in its revision prior to submission – KMM, MT, MRM.

This work was funded by a British Heart Foundation (BHF) programme grant (RG/11/7/28916). AFW was a BHF funded PhD student.

This article has an online data supplement, which is accessible from this issue's table of content online at www.atsjournals.org

Abstract

Rationale: The incidence of pulmonary arterial hypertension (PAH) is greater in women suggesting estrogens may play a role in the disease pathogenesis. Experimentally, in males, exogenously administered estrogen can protect against PH. However, in models that display female susceptibility, estrogens may play a causative role.

Objectives: To clarify the influence of endogenous estrogen and gender in PH and assess the therapeutic potential of a clinically available aromatase inhibitor.

Methods: We interrogated the effect of reduced endogenous estrogen in males and females using the aromatase inhibitor, anastrozole, in two models of PH; the hypoxic mouse and Sugen 5416/hypoxic rat. We also determined the effects of gender on pulmonary expression of aromatase in these models and in lungs from PAH patients.

Results: Anastrozole attenuated PH in both models studied, but only in females. To verify this effect was due to reduced estrogenic activity we confirmed that in hypoxic mice inhibition of estrogen receptor alpha also has a therapeutic effect specifically in females. Female rodent lung displays increased aromatase and decreased BMPR2 and Id1 expression compared to male. Anastrozole treatment reversed the impaired BMPR2 pathway in females. Increased aromatase expression was also detected in female human pulmonary artery smooth muscle cells compared to male.

Conclusions: The unique phenotype of female pulmonary arteries facilitates the therapeutic effects of anastrozole in experimental PH confirming a role for endogenous estrogen in the disease pathogenesis in females and suggests aromatase inhibitors may have therapeutic potential.

Word count: 238 ***Keywords***: pulmonary hypertension, estrogen, gender.

Introduction

Pulmonary arterial hypertension (PAH) is characterised by severe pulmonary arterial remodelling and occlusive pulmonary vascular lesions, leading to right ventricular failure. Epidemiological studies report a greater incidence of the disease in females; depending on the disease classification the female to male ratio can be as great as 4:1 (1, 2). The female predisposition to PAH has given rise to the hypothesis that female sex hormones, primarily estrogens, may play a causative role in the development of the condition (3). However, the role of estrogen in PAH remains controversial.

The majority of preclinical studies into the role of estrogens in PH have utilised male animals (4-6) and describe protective effects of estrogen when administered exogenously. However, there is compelling evidence that endogenous estrogen may contribute to the pathogenesis of PH. Recently, we have described novel murine models where only female animals develop PH such as mice over-expressing the serotonin transporter gene (SERT+ mouse) (7) and Mts1(8). In these models the predominant circulating estrogen 17β-estradiol plays an essential role in the development of the PH phenotype (7-9). Estrogen can also induce proliferation of human pulmonary artery smooth muscle cell (hPASMCs) and may therefore contribute to the pulmonary artery remodelling observed in PAH (7, 10).

One explanation of the current controversies is that there are gender differences in the influence of endogenous estrogens on the pathophysiology of PH. Determining any gender differences in pulmonary responses to estrogen is vitally important for understanding the nature and origins of PAH. To our knowledge, there have been no comprehensive male *versus* female comparative studies into the role of *endogenous* estrogen in the pulmonary circulation.

Aromatase (CYP19A1), a member of the cytochrome P450 superfamily, synthesizes estrogens through the aromatization of androgens. In pre-menopausal women estrogen synthesis occurs mainly in the ovarian follicles and corpus luteum, but also to a lesser extent in non-glandular tissues such as adipose tissue and liver. In postmenopausal women and men, adipose tissue is a major source of estrogen (11). Little is known of the role aromatase plays within the pulmonary circulation. Therefore, to characterise the role of endogenous estrogen in PAH, the effects of an aromatase inhibitor were studied in two models of PH in male and female animals. We also assessed aromatase expression in the lung tissue of these animal models and in lung samples from PAH patients.

Methods

An expanded methods section is available in the Online Supplement

Hypoxic Studies

The ability of anastrozole to reduce progression of, and reverse, established PH in hypoxic mice was assessed. Hypoxic PH in C57BL/6 mice was achieved with 14 days hypoxia as described previously (10, 12). Mice were then maintained in hypoxic conditions for a further 14 days during which time the aromatase inhibitor, anastrozole was administered (Tocris) 0.3 $mgkg^{-1}$ or 3 $mgkg^{-1}$ or vehicle (1% carboxymethylcellulose) daily (s.c.). Another cohort of mice were administered with an ER± antagonist, MPP 2 $mgkg^{-1}day^{-1}$ for 14days (s.c.). Age-matched mice housed in normoxic conditions were studied as controls. See online supplement for ethical considerations and housing details.

Sugen 5416 + hypoxia (Su/Hx) Study

The ability of anastrozole to reduce progression of, and reverse, established PH was also assessed in the rat model of hypoxia + Sugen5416 (Su) as described in detail in online supplement. Briefly, Wistar Kyoto rats were given a single injection of Su 20mgkg^{-1} (s.c.) or 0.9% (s.c.) saline and exposed to hypoxia for 14 days then retained in normoxia for two weeks during which time they were dosed with anastrozole (0.03, 0.3 or 3 mgkg^{-1}day^{-1}) or vehicle (1% carboxymethylcellulose) orally.

Hemodynamic Measurements

Heart rate, right ventricular systolic pressure (RVSP), systemic arterial pressure and cardiac output were measured and analyzed as previously described (10, 12, 13). See online supplement for details.

Right Ventricular Hypertrophy

Right ventricular hypertrophy (RVH) was assessed by weighing the right ventricular free wall and left ventricle plus septum. The ratio expressed as RV/LV+S. See online supplement for details.

Lung Histopathology

3µm lung sagittal sections were stained with ±-smooth-muscle actin (<80 µm external diameter) and microscopically assessed for degree of muscularisation in a blinded fashion, as previously described (14) and in online supplement.

qRT-PCR

mRNA expression was assessed in lungs of mice by qRT-PCR as described previously and in online supplement (10).

Immunoblotting

Protein expression was assessed by immunoblotting in lung and hPASMCs as described previously and in online supplement (10).

Lung Immunolocalization

Aromatase expression was investigated in murine, rat and human lung by immunohistochemistry as described previously and in online supplement (10).

Measurement of Estradiol Concentrations.

Circulating estradiol was quantified in plasma by ELISA (Estradiol ELISA, Life Technologies).

hPASMCs and PAH-PASMCs

hPASMCs were prepared and cultured as described previously and in online supplement (10).

Statistics

All data are expressed as mean ± SEM. Data were analysed using one-way ANOVA with Dunnett's or Bonferroni post-hoc analyses and Student's unpaired t-test (as appropriate and indicated in figure legends) using GraphPad Prism 5 software. A P value < 0.05 was considered statistically significant.

Results

Inhibition of aromatase attenuates experimental PH in female but not male mice.

In female mice anastrozole reduced hypoxia-induced increases in RVSP, RVH and pulmonary vascular remodelling (PVR) (Figure 1A-D). However, in male mice, anastrozole when used at the most effective dose ($3mgkg^{-1}day^{-1}$) had no significant effect on hypoxia-induced elevations in RVSP, RVH or PVR (Figure 1E-H). Anastrozole had no significant effect on mean systemic arterial blood pressure or heart rate (Figure E1 online supplement).

To confirm that this effect was not due to any off-target effects of anastrozole, the effect of MPP, an ER± antagonist was assessed. MPP was selected as ER± protein levels were found to be significantly elevated in pulmonary arteries from female hypoxic mice, whilst ER² was significantly reduced. No significant differences in the expression of ER± or ER² were observed in pulmonary arteries from male mice (Figure E2 online supplement). MPP markedly attenuated hypoxia-induced increases in RVSP and PVR in females but had no therapeutic effect in males (Figure E3 online supplement).

In female Su/Hx rats anastrozole reduced increases in RVSP, RVH, PVR and reversed the development of occlusive vascular lesions (Figure 2A-E). In contrast to females, anastrozole had no significant effect on Su/Hx-induced changes in RVSP, RVH or PVR in male animals (Figure 3A-E).

Cardiac and pulmonary function were assessed by echocardiography. In female rats anastrozole had no effect on cardiac output, but did slightly restore decreased pulmonary artery acceleration time (PAAT) (Figure E4 online supplement). In Su/Hx

male rats anastrozole had no effect on cardiac output or PAAT (Figure E4 online supplement).

Aromatase expression in hypoxic and Su/Hx-induced PH.

Weak aromatase expression was observed in pulmonary arteries from normoxic mice whilst expression was abundant in hypoxic mice, localising to the smooth muscle layer (Figure 4A). Analysis of whole lung tissue by immunoblotting showed that female mice express significantly higher levels of aromatase protein in whole lung compared to male in both normoxic and hypoxic conditions (Figure 4B). Similarly, in pulmonary arteries from normoxic rats negligible to weak aromatase staining was observed whilst expression was abundant in arteries from Su/Hx rats, localising within the vascular smooth muscle (Figure 5A). Aromatase staining was absent from the endothelial layer of rat pulmonary arteries (Figure 5B). In addition, aromatase was absent from endothelial cells within the small occlusive vascular lesions observed in Su/Hx rat lung (Figure 5C). Male rats also express significantly lower aromatase protein levels in the whole lung compared to female under both normoxic and Su/Hx conditions (Figure 5D). Exposure to Su/Hx had no effect on aromatase expression in female or male rat lung when compared to normoxic control (Figure 5D).

Aromatase expression in human lung.

Aromatase was found to be expressed in pulmonary arteries of control, female PAH and male PAH patients localising mainly within the smooth muscle layer (Figure 6A). Aromatase immunostaining was also present in vascular lesions from PAH patients (Figure 6B) also localising to the smooth muscle layer. Aromatase immunoreactivity

was absent in the endothelium of most PAH patients regardless of BMPR2 status (Figure 6B and E5B). In addition, there was no evidence of aromatase expression in human microvascular pulmonary artery endothelial cells (hMPAECs) (Figure E5C online supplement). PASMCs isolated from control postmenopausal females express significantly higher levels of aromatase than those from males (Figure 6C), however, no significant difference in aromatase expression in PASMCs from female control *versus* female PAH patients was observed (Figure 6D).

Effect of anastrozole on circulating estrogen levels.

Anastrozole 0.3mgkg^{-1} and 3mgkg^{-1} decreased levels of circulating estradiol, the major bioactive estrogen in female mice and had no effect on circulating estrogen levels in the male mice. Furthermore, hypoxia alone had no effect of circulating estrogen levels in either female or male mice (Figure 7A)

In the Su/Hx rat model, estradiol levels were undetectable in male rats. However, in female rats, circulating estradiol levels were found to be significantly elevated in the Su/Hx rats compared to normoxic controls (Figure 7B). Anastrozole reduced circulating estradiol levels in a dose-dependent fashion. Analysis across the female Su/Hx treatment groups revealed a significant correlation between circulating estradiol concentrations and RVH (Figure 7C) as well as the percentage of muscularised pulmonary arteries (Figure 7D).

Effects of anastrozole on hypoxia and Su/Hx-mediated changes in bone morphogenetic protein receptor 2 (BMPR2).

In normoxic conditions lung transcript levels of BMPR2 were significantly lower in female mice than male. Administration of anastrozole resulted in a significant

upregulation of BMPR2 in female lung, restoring levels to that of males whilst having no effect on BMPR2 levels in male lung (Figure 8A). In hypoxia, BMPR2 transcript and protein levels were significantly reduced in both male and female lung. Anastrozole treatment restored the hypoxia-mediated downregulation in BMPR2 in females (Figure 8A-B) but not males (Figure 8A&C). In the Su/Hx rat model, BMPR2 transcript was also found to be significantly decreased in both male and female lung compared to normoxic controls (Figure 8D-F). This effect was reversed in female rats treated with anastrozole $3mgkg^{-1}day^{-1}$ (Figure 8D-E) but not male rats (Figure 8F). The male rats had significantly higher normoxic transcript levels of BMPR2 compared to females, consistent with our observations in mice (Figure 8D).

Female normoxic mouse and rat lung demonstrated significantly lower levels of Id1 and Id3 (Figure E6 online supplement) than males. In females anastrozole significantly elevated Id1 and Id3 to levels similar to that observed in males but had no effect on Id1 and Id3 expression in male lung. Id1 expression was significantly reduced in both male and female disease models, whilst Id3 was specifically downregulated in males. The PH-mediated decreases in Id1 were rescued by administration of anastrozole in female animals but not male (Figure E6 online supplement). ER± antagonist MPP also restored hypoxia-mediated reductions in BMPR2 and Id1 (Figure E7 online supplement).

Discussion

Increased synthesis of estrogen has been clinically associated with porto-pulmonary hypertension (15) and estrogen is causative in female susceptible models of PH (7-

9). Studies into the role of estrogen in PAH have failed to reach a concensus, mainly due to the variety of experimental approaches adopted. Indeed, many experimental studies have demonstrated a protective effect of estrogen in male animals (4-6). These valuable studies examined the influence of estrogen administered to males where estrogen levels are normally extremely low or undetectable. In addition, these studies utilise intact males, hence the presence of high endogenous testosterone combined with high circulating estrogen levels (due to the exogenously added estradiol) are not a state that would normally occur physiologically and may influence interpretation of results. In the instance of monocrotaline (MCT)-induced PH the beneficial effects of estrogen may be owing to the fact that MCT is a toxin reported to cause gonadal toxicity and reduce estrogen levels (16). In our experimental design we wished to compare males and females and address a different question: 'what is the role of *endogenous* estrogen and is it different in intact males and females'?

The data presented in this study explains some of these current controversies by providing several unique insights into the influence of gender and endogenous estrogen in the development of PH. We demonstrate that endogenous estrogen contributes to the pathophysiology of PH in females and that there is potential for local estrogen synthesis in PASMCs. Given the previously demonstrated mitogenic effects of estrogen in PASMCs (7), we also describe a unique pro-proliferative phenotype in female PASMCs owing to elevated aromatase and reduced BMPR2 and Id1 expression.

Using anastrozole we inhibited the enzyme aromatase, which is responsible for estrogen synthesis, to determine the role of endogenous estrogen on established PH in females and males. Anastrozole reduced plasma estrogen and attenuated hypoxia and Su/Hx-induced changes in RVSP, RVH and PVR in females.

Furthermore, in the female Su/Hx model a positive correlation between circulating estrogen concentrations and disease severity was established, suggesting the therapeutic effects of anastrozole were related to a decrease in plasma estrogen levels. In the males, there was no therapeutic effect of anastrozole; plasma estrogen was below the level of detection and unaffected by anastrozole.

We also demonstrated that there is a dysregulation in the expression of estrogen receptors in hypoxic female mice but not male, with ER± expression significantly increased and ER² decreased in female pulmonary artery whilst both receptors remain unaffected in males. Furthermore, we show that an ER± antagonist, MPP, has selective therapeutic effect in female hypoxic mice, not male. This corroborates our hypothesis that endogenous estrogen is pathogenic in female models of PH. Anastrozole is a third generation highly selective competitive inhibitor of aromatase and as such has few off-target actions. Preclinical studies show that even when used up to doses of $10mgkg^{-1}$ in rats no reported disturbances in adrenal steroidogenesis were observed (17).

Estrogen is widely described to be cardioprotective due to its direct action on the heart. Epidemiological evidence shows that pre-menopausal women have a lower risk for mortality from cardiovascular diseases than men (18-20). Given the cardioprotective effects of estrogen there is concern that treatment with aromatase inhibitors may facilitate right ventricular dysfunction. Hence we interrogated the influence of anastrozole on heart function in the Su/Hx rat model by echocardiography. Anastrozole had no detrimental effects on cardiac output or pulmonary artery acceleration time in rats. These findings suggest that depletion of estrogen is not having detrimental effects on the heart that might limit the use of anastrozole in the treatment of PAH. Aromatase inhibitors are currently widely

prescribed to patients with estrogen receptor-sensitive breast cancer and many systemic side-effects have been investigated Available data do not support an association between aromatase inhibitors and an increased risk of cardiovascular disease, PAH or a deleterious effect on lipid metabolism in humans (21).

Aromatase was expressed in small pulmonary arteries of both female and male rodents localising within the smooth muscle layer. However, aromatase expression was significantly higher in the lungs from female rats and mice than males. This may partially explain the increased therapeutic effect of anastrozole in the females. We also verified that aromatase is expressed in the smooth muscle of pulmonary arteries in human lung, demonstrating that aromatase is abundantly expressed in vascular smooth muscle from control non-PAH lung sections and in complex vascular lesions. This coupled with the elevated aromatase expression observed in female PASMCs suggests female PASMCs have the ability to synthesis higher levels of estradiol that male. This may contribute to the female susceptibility to PAH given the mitogenic properties of estradiol.

This is the first study to report that there is the potential for local estrogen production in pulmonary arteries. We could find no evidence for aromatase expression in the endothelium of rats, mice or human in our studies regardless of their disease status. Likewise, hMPAECs do not express aromatase. This suggests that estrogen produced by PASMCs that exerts a paracrine proliferative effect on adjacent PASMCs. Indeed, we have previously demonstrated that estrogen induces proliferation in human PASMCs (7, 8). Estrogen synthesized within extragonadal compartments has been postulated to act at a local tissue level in a paracrine fashion (22). Thus, the total amount of estrogen synthesized by these extragonadal sites may be small but the local tissue concentrations achieved high enough to exert

significant biologic influence locally (11). Given the expression of aromatase in the smooth muscle layer of the pulmonary artery the local concentration of estrogen in the pulmonary artery may be much greater than circulating concentrations. Estrogen levels will also be affected by metabolism. We have previously shown that expression of cytochrome P450 1B1 (CYP1B1) an estrogen metabolising enzyme is dysregulated in the Su/Hx mouse model of PH (10). Differences in estrogen metabolism between the hypoxic mouse model and Su/Hx rat model of PH may explain why circulating estrogen levels are elevated in Su/Hx rats but not hypoxic mice.

Loss of function associated with BMPR2 mutations in PAH results in reduction of the growth inhibitory effects of BMPs, facilitating the proliferation of PASMCs and contributing to pulmonary vascular remodelling (23). BMPR2 is also often observed to be down-regulated in animal models of PAH (24, 25). Here we showed that expression of BMPR2 and its downstream mediator Id1 are significantly decreased in the lungs of normoxic female rodents compared with males. The significantly lower levels of BMPR2 and Id1 in females can be restored to levels similar to that observed in males by anastrozole, suggesting estrogen may be responsible for the suppressed BMPR2 signaling axis in females. Furthermore, anastrozole treatment restored hypoxic and Su/Hx-mediated reductions in BMPR2 mRNA and protein levels in female rodents whilst having no effect on males. These observations provide one further explanation for the selective therapeutic effect of anastrozole on the development of PH in female models, i.e. endogenous estrogen in the lungs of females is greater due to increased aromatase expression; this combined with the effects of hypoxia or Su/Hx, decreases expression of BMPR2 which is already

significantly reduced in females. Consequently anastrozole, by decreasing endogenous estrogen levels, has a selective therapeutic effect in females.

In hPAH families, penetrance of PAH in BMPR2 mutation carriers is low, suggesting other risk factors must influence the emergence of the PAH phenotype. Indeed, further predisposing genes such as KCNK3 and TOPBP4 have been recently identified (26, 27). Whilst increased aromatase expression combined with decreased BMPR2 signaling may predispose susceptible females to PAH it is unlikely that these factors alone are responsible for the clinical presentation of disease in all females; and clearly males develop PAH, displaying poorer survival rates than females (1). Our results suggest that once the disease is established, the increased influence of both circulating and locally produced estrogen in women, results in an enhanced pathogenic effect on the pulmonary circulation compared to males. Consistent with this, female PAH patients have 2.8-fold higher number of plexiform lesions compared with their male counterparts (20).

However, in some patient sub-groups including PAH associated with HIV, sleep apnea and portopulmonary hypertension the prevalence of PAH is greater in males (1). However, these primary conditions occur more frequently in men, potentially influencing the male:female ratio of those developing PAH (e.g.(28-30)). In addition, estrogen may contribute to the disease pathophysiology in males within these subgroups. For instance, in HIV dysregulation in sex hormone concentrations have been reported in both sexes. In one study estradiol was reported to significantly increase over an 18 month period in male HIV patients (31). Furthermore, obstructive sleep apnea is most common in obese men (29), in which elevated circulating estrogen levels are common due to the high expression and activity of aromatase within adipose tissue (32, 33). Polymorphisms in the aromatase gene

have also been associated with increased risk of portopulmonary hypertension in patients with liver disease. These polymorphisms are associated with increased estradiol production, supporting a functional effect of aromatase activity in both male and female patients (15). Thus, elevated estrogen is observed in the males in these PAH subgroups. This is not incompatible with the suggestion that when elevated, endogenous estrogen may contribute to the pathobiology PAH in males as well as females.

The results of this study also suggests that non-estrogenic contraceptives be recommended to pre-menopausal PAH patients, although these are already contra-indicated for PAH patients due to the increased risk of venous thromboembolic disease (34).

In summary, we have demonstrated that endogenous estrogen plays a causative role in the development of experimental PH in female animal models of the disease. Inhibition of aromatase with anastrozole reduces moderate and severe experimental PH in female animals via reduction in endogenous estrogen. The reason for the sexual dimorphism in the therapeutic effects of anastrozole may be due to a unique phenotype of female pulmonary arteries. We propose that increased capability of female PASMCs to produce estrogen locally via aromatase contributes to a reduction in the BMPR2 signalling axis and may contribute to the pathology and increased incidence of the disease in females. The results partly explain the 'estrogen paradox' and suggest that aromatase inhibitors may have therapeutic potential in the treatment of PAH in females.

Acknowledgments

We are grateful to Professor N. W. Morrell (University of Cambridge) for providing human lung tissue and Valerie Khambata (Novartis Institutes of BioMedical Research) for technical assistance.

References

1. Shapiro S, Traiger GL, Turner M, McGoon MD, Wason P, Barst RJ. Sex differences in the diagnosis, treatment, and outcome of patients with pulmonary arterial hypertension enrolled in the registry to evaluate early and long-term pulmonary arterial hypertension disease management. *Chest* 2012;141:363-373.

2. McGoon MD, Benza RL, Escribano-Subias P, Jiang X, Miller DP, Peacock AJ, Pepke-Zaba J, Pulido T, Rich S, Rosenkranz S, Suissa S, Humbert M. Pulmonary arterial hypertension: Epidemiology and registries. *J Am Coll Cardiol* 2013;62:D51-59.

3. Rabinovitch M. Molecular pathogenesis of pulmonary arterial hypertension. *J Clin Invest* 2012;122:4306-4313.

4. Lahm T, Albrecht M, Fisher AJ, Selej M, Patel NG, Brown JA, Justice MJ, Brown MB, Van Demark M, Trulock KM, Dieudonne D, Reddy JG, Presson RG, Petrache I. 17beta-estradiol attenuates hypoxic pulmonary hypertension via estrogen receptor-mediated effects. *Am J Respir Crit Care Med* 2012;185:965-980.

5. Umar S, Iorga A, Matori H, Nadadur RD, Li J, Maltese F, van der Laarse A, Eghbali M. Estrogen rescues preexisting severe pulmonary hypertension in rats. *Am J Respir Crit Care Med* 2011;184:715-723.

6. Xu DQ, Luo Y, Liu Y, Wang J, Zhang B, Xu M, Wang YX, Dong HY, Dong MQ, Zhao PT, Niu W, Liu ML, Gao YQ, Li ZC. Beta-estradiol attenuates hypoxic pulmonary hypertension by stabilizing the expression of p27kip1 in rats. *Respir Res* 2010;11:1465-9921.

7. White K, Dempsie Y, Nilsen M, Wright AF, Loughlin L, MacLean MR. The serotonin transporter, gender, and 17 beta oestradiol in the development of pulmonary arterial hypertension. *Cardiovasc Res* 2011;90:373-382.

8. Dempsie Y, Nilsen M, White K, Mair KM, Loughlin L, Ambartsumian N, Rabinovitch M, MacLean MR. Development of pulmonary arterial hypertension in mice over-expressing s100a4/mts1 is specific to females. *Resp Res* 2011;12.

9. Dempsie Y, Macritchie NA, White K, Morecroft I, Wright AF, Nilsen M, Loughlin L, Mair KM, Maclean MR. Dexfenfluramine and the oestrogen-metabolizing enzyme cyp1b1 in the development of pulmonary arterial hypertension. *Cardiovasc Res* 2013;99:24-34.

10. White K, Johansen AK, Nilsen M, Ciuclan L, Wallace E, Paton L, Campbell A, Morecroft I, Loughlin L, McClure JD, Thomas M, Mair KM, MacLean MR. Activity of the estrogen-metabolizing enzyme cytochrome p450 1b1 influences the development of pulmonary arterial hypertension. *Circulation* 2012;126:1087-U1202.

11. Simpson ER, Clyne C, Rubin G, Boon WC, Robertson K, Britt K, Speed C, Jones M. Aromatase - a brief overview. *Annu Rev Physiol* 2002;64:93-127.

12. Dempsie Y, Morecroft I, Welsh DJ, MacRitchie NA, Herold N, Loughlin L, Nilsen M, Peacock AJ, Harmar A, Bader M, MacLean MR. Converging evidence in support of the serotonin hypothesis of dexfenfluramine-induced pulmonary hypertension with novel transgenic mice. *Circulation* 2008;117:2928-2937.

13. Ciuclan L, Bonneau O, Hussey M, Duggan N, Holmes AM, Good R, Stringer R, Jones P, Morrell NW, Jarai G, Walker C, Westwick J, Thomas M. A novel murine model of severe pulmonary arterial hypertension. *Am J Resp Crit Care* 2011;184:1171-1182.

14. Keegan A, Morecroft I, Smillie D, Hicks MN, MacLean MR. Contribution of the 5-ht1b receptor to hypoxia-induced pulmonary hypertension - converging evidence using 5-ht1b-receptor knockout mice and the 5-ht1b/1d-receptor antagonist gr127935. *Circ Res* 2001;89:1231-1239.

15. Roberts KE, Fallon MB, Krowka MJ, Brown RS, Trotter JF, Peter I, Tighiouart H, Knowles JA, Rabinowitz D, Benza RL, Badesch DB, Taichman DB, Horn EM, Zacks S, Kaplowitz N, Kawut SM, Dis PVCL. Genetic risk factors for portopulmonary hypertension in patients with advanced liver disease. *Am J Resp Crit Care* 2009;179:835-842.

16. Tofovic SP, Jackson EK. Complexities of oestradiol pharmacology in pulmonary arterial hypertension. *Eur Respir J* 2013;41:1465-1466.

17. Dukes M, Edwards PN, Large M, Smith IK, Boyle T. The preclinical pharmacology of "arimidex" (anastrozole; zd1033)--a potent, selective aromatase inhibitor. *The Journal of steroid biochemistry and molecular biology* 1996;58:439-445.

18. Barrett-Connor E. Sex differences in coronary heart disease. Why are women so superior? The 1995 ancel keys lecture. Circulation. 1997 Jan 7;95(1):252-64.; 1997.

19. Silber DH. Heart failure in women. *Curr Womens Health Rep* 2003;3:104-109.

20. Robertson T, Kennard ED, Mehta S, Popma JJ, Carrozza JP, Jr., King SB, 3rd, Holmes DR, Cowley MJ, Hornung CA, Kent KM, Roubin GS, Litvack F, Moses JW, Safian R, Desvigne-Nickens P, Detre KM. Influence of gender on in-hospital clinical and angiographic outcomes and on one-year follow-up in the new approaches to coronary intervention (naci) registry. *Am J Cardiol* 1997;80:26K-39K.

21. Perez EA. Safety profiles of tamoxifen and the aromatase inhibitors in adjuvant therapy of hormone-responsive early breast cancer. *Annals of oncology : official journal of the European Society for Medical Oncology / ESMO* 2007;18 Suppl 8:viii26-35.

22. Labrie F, Luu-The V, Lin SX, Labrie C, Simard J, Breton R, Belanger A. The key role of 17 beta-hydroxysteroid dehydrogenases in sex steroid biology. *Steroids* 1997;62:148-158.

23. Yang J, Davies RJ, Southwood M, Long L, Yang X, Sobolewski A, Upton PD, Trembath RC, Morrell NW. Mutations in bone morphogenetic protein type ii receptor cause dysregulation of id gene expression in pulmonary artery smooth muscle cells: Implications for familial pulmonary arterial hypertension. *Circ Res* 2008;102:1212-1221.

24. Takahashi H, Goto N, Kojima Y, Tsuda Y, Morio Y, Muramatsu M, Fukuchi Y. Downregulation of type ii bone morphogenetic protein receptor in hypoxic pulmonary hypertension. *American journal of physiology Lung cellular and molecular physiology* 2006;290:L450-458.

25. Long L, Crosby A, Yang X, Southwood M, Upton PD, Kim DK, Morrell NW. Altered bone morphogenetic protein and transforming growth factor-beta signaling in rat models of pulmonary hypertension: Potential for activin receptor-like kinase-5 inhibition in prevention and progression of disease. *Circulation* 2009;119:566-576.

26. de Jesus Perez VA, Yuan K, Lyuksyutova MA, Dewey F, Orcholski ME, Shuffle EM, Mathur M, Yancy L, Jr., Rojas V, Li CG, Cao A, Alastalo TP, Khazeni N, Cimprich KA, Butte AJ, Ashley E, Zamanian RT. Whole exome sequencing reveals topbp1 as a novel gene in idiopathic pulmonary arterial hypertension. *Am J Respir Crit Care Med* 2014.

27. Girerd B, Perros F, Antigny F, Humbert M, Montani D. Kcnk3: New gene target for pulmonary hypertension? *Expert Rev Respir Med* 2014.

28. Popovic RM, White DP. Upper airway muscle activity in normal women: Influence of hormonal status. *J Appl Physiol (1985)* 1998;84:1055-1062.

29. Muxfeldt ES, Margallo VS, Guimarães GM, Salles GF. Prevalence and associated factors of obstructive sleep apnea in patients with resistant hypertension. *American journal of hypertension* 2014.

30. Presanis AM, Gill ON, Chadborn TR, Hill C, Hope V, Logan L, Rice BD, Delpech VC, Ades AE, De Angelis D. Insights into the rise in hiv infections, 2001 to 2008: A bayesian synthesis of prevalence evidence. *AIDS* 2010;24:2849-2858.

31. Teichmann J, Schmidt A, Lange U, Stracke H, Discher T, Friese G, Lohmeyer J, Bretzel RG. Longitudinal evaluation of serum estradiol and estrone in male patients infected with the human immunodeficiency virus. *European journal of medical research* 2003;8:77-80.

32. SCHNEIDER G, KIRSCHNER MA, BERKOWITZ R, ERTEL NH. Increased estrogen production in obese men. *The Journal of Clinical Endocrinology & Metabolism* 1979;48:633-638.

33. Zumoff B, Strain GW, Kream J, O'Connor J, Levin J, Fukushima DK. Obese young men have elevated plasma estrogen levels but obese premenopausal women do not. *Metabolism: clinical and experimental* 1981;30:1011-1014.

34. Plu-Bureau G, Hugon-Rodin J, Maitrot-Mantelet L, Canonico M. Hormonal contraceptives and arterial disease: An epidemiological update. *Best practice & research Clinical endocrinology & metabolism* 2013;27:35-45.

Figure 1

Inhibition of aromatase attenuates chronic hypoxia-induced PH in female mice. **Female mice:** Effects of the aromatase inhibitor, anastrozole (ANA) 0.3 $mgkg^{-1}day^{-1}$ and 3 $mgkg^{-1}day^{-1}$ for 14 days on (**A**) RVSP (n=8-10 per group), (**B**) RVH (n=8-10 per group) (as determined by RV/LV+S ratio) and (**C**) the % of remodelled pulmonary arteries in normoxic mice and hypoxic female mice with established PH (n=6 per group). (**D**) Representative images of pulmonary arteries from normoxic and hypoxic female mice treated with or without anastrozole 3 $mgkg^{-1}day^{-1}$ (brown staining indicates ±-smooth muscle actin; scale bar (**-**) indicates 20µm). **Male mice:** Effects of ANA 3 $mgkg^{-1}day^{-1}$ for 14 days on (**E**) RVSP (n=8-10 per group), (**F**) RVH (n=8-10 per group) (as determined by RV/LV+S ratio) and (**G**) the % of remodelled pulmonary arteries in normoxic mice and hypoxic male mice with established PH (n=6 per group). (**H**) Representative images of pulmonary arteries from normoxic and hypoxic male mice treated with or without anastrozole 3 $mgkg^{-1}day^{-1}$ (brown staining indicates ±-smooth muscle actin; scale bar (**-**) indicates 20µm). Data displayed as mean ± SEM. **p<0.01 and ***p<0.001 as indicated, determined by one-way ANOVA with Bonferroni post test. RVSP = right ventricular systolic pressure, RVH = right ventricular hypertrophy and RV/LV+S = right ventricle/left ventricle + septum.

Figure 2

Inhibition of aromatase attenuates Su5416/hypoxia (Su/Hx)-induced PH in female rats. (**A**) RVSP (n=5-8 per group), (**B**) RVH (n=5-8 per group) (as determined by RV/LV+S) and (**C**) the % remodelled pulmonary arteries (n=5-8 per group) were assessed on day 14 (D14) and day 28 (D28) following administration of Su/Hx in female rats treated with or without anastrozole (ANA) 0.03 $mgkg^{-1}day^{-1}$, 0.3 $mgkg^{-1}day^{-1}$ or 3 $mgkg^{-1}day^{-1}$ for 14 days in female rats (from D14-28). Representative images showing (**D**) ±-smooth muscle actin (±-SMA) staining in pulmonary arteries from Su/Hx female rats treated with or without anastrozole (±-SMA = brown staining; scale bar (**-**) indicates 20µm). (**E**) The percentage of pulmonary arteries which are fully occluded in female rats treated with or without anastrozole (n=5-8) and (**F**) representative image of an occluded pulmonary artery (±-SMA = pink, vWF = black; scale bar (**-**) indicates 20µm). Data displayed as mean ± SEM. * p<0.05, **p<0.01 and ***p<0.001 as indicated, # p<0.01 versus D14 Su/Hx as determined by one-way ANOVA with Dunnett's post test. RVSP = right ventricular systolic pressure and RVH = right ventricular hypertrophy.

Figure 3

Inhibition of aromatase does not attenuate Su5416/hypoxia (Su/Hx)-induced PH in male rats. (A) RVSP (n=5-8 per group), (B) RVH (n=5-8 per group) and (C) the % remodelled pulmonary arteries (n=5-8 per group) were assessed on day 14 (D14) and day 28 (D28) following administration of Su/Hx in male rats treated with or without anastrozole (ANA) 3 $mgkg^{-1}$ (from D14-28) Representative images showing (D) ±-SMA staining in pulmonary arteries from SU/Hx male rats treated with or without anastrozole (±-SMA = brown; scale bar (-) indicates 20µm). (E) The percentage of pulmonary arteries which are fully occluded (n=5-8 per group) in male rats treated with or without anastrozole $3mgkg^{-1}$ and (F) representative image of an occluded pulmonary artery (±-SMA = pink, vWF = black ; scale bar (-) indicates 10µm). Data displayed as mean ± SEM. * $p<0.05$, ** $p<0.01$ and *** $p<0.001$ as indicated, determined by one-way ANOVA with Dunnett's post test. RVSP = right ventricular systolic pressure and RVH = right ventricular hypertrophy .

Figure 4

Effect of chronic hypoxia on aromatase expression in mouse pulmonary artery and whole lung. Representative images showing (**A**) aromatase immunolocalisation in pulmonary arteries (scale bar (**-**) indicates 20µm) with 3µm consecutive sections showing ±-smooth muscle actin (±-SMA) and von Willebrand factor (vWF) (representative of n=4 per group, brown staining). For IgG control see online supplement Figure E5. (**B**) Representative immunoblot and quantification of aromatase protein expression in whole lung from normoxic and hypoxic, female and male mice (n=5-6 per group). Data displayed as mean ± SEM. *p<0.05 and ** p<0.01 as indicated, determined by one-way ANOVA with Bonferroni post test.

Figure 5

Effect of Su5416/hypoxia (Su/Hx) on aromatase expression in rat pulmonary artery and whole lung. Representative images showing (**A**) aromatase immunolocalisation in pulmonary arteries (scale bar (**-**) indicates 20µm) with 3µm consecutive sections showing ±-smooth muscle actin (±-SMA) and von Willebrand factor (vWF) (representative of n=4 per group, brown staining) (for IgG control refer to online supplement Figure E5. (**B**) Representative image showing the absence of aromatase immunolocalisation in the endothelial layer of rat pulmonary artery (scale bar (**-**) indicates 50µm (x400 magnification)) with 3µm consecutive sections showing ±-smooth muscle actin (±-SMA) and von Willebrand factor (vWF) (brown staining). (**C**) Representative image showing aromatase immunolocalisation in small occlusive vascular lesions from SuHx rat (scale bar (**-**) indicates 20µm) with 3µm consecutive sections showing ±-smooth muscle actin (±-SMA) and von Willebrand factor (vWF) (brown staining). (**D**) Representative immunoblot and quantification of aromatase protein expression in whole lung from normoxic and hypoxic, female and male rats (n=5-6 per group). Data displayed as mean ± SEM. *p<0.05 and ** p<0.01 as indicated, determined by one-way ANOVA with Bonferroni post test.

Figure 6

Aromatase expression in human PAH. (**A**) Representative images showing aromatase immunolocalisation in control and female and male PAH patients. (**B**) Representative images showing examples of aromatase immunolocalisation in vascular lesions from PAH patients (aromatase (AROM) = pink; ±-smooth muscle actin (±-SMA) and von Williebrand factor (vWF) = brown; scale bar (**-**) indicates 100µm; for IgG control see online supplement Figure E5). Aromatase protein expression was also assessed by immunoblotting using human pulmonary artery smooth muscle cells (hPASMCs). (**C**) Representative immunoblots and graph showing quantification comparing aromatase expression in hPASMCs isolated from male and female control (n=4 samples per group) and (**D**) female control and female PAH patients (n=4 samples per group). Data displayed as mean ± SEM. ***p<0.001 as indicated, determined by two-tailed, unpaired t-test. **1-11, a,e,i** and **j** correspond to patient information on human tissues and cells referred to in online supplement Table E3.

Figure 7

Effect of aromatase inhibition on circulating estradiol (E2) levels in models of pulmonary hypertension. (**A**) Circulating plasma E2 levels in normoxic and hypoxic female and male mice treated with or without anastrozole (ANA) for 14 days (n=5 per group)**.** Data displayed as mean ± SEM. *p<0.05, **p<0.01 and ** p<0.001 as indicated, determined by one-way ANOVA with Bonferroni post test. (**B**) Circulating E2 levels in female Su/Hx rats treated with or without 0.3 $mg^{-1}kg^{-1}day^{-1}$, 1 $mg^{-1}kg^{-1}day^{-1}$ or 3 $mg^{-1}kg^{-1}day^{-1}$ anastrozole (n=4-5 per group). Data displayed as mean ± SEM. *p<0.05 and *** p<0.001 as indicated, determined by one-way ANOVA with Dunnett's post test. Plasma E2 levels from female Su/Hx rats were used to determine if there was any correlation with disease severity using Pearson's coefficient. Significant correlation between plasma E2 levels and (**C**) RVH (as determined by RV/LV+S) (n=30) and (**D**) the percentage of muscularised pulmonary arteries (n=30). *p<0.05 and **p<0.01 as indicated. All E2 concentrations are expressed as a percentage relative to normoxic set at 100%.

Figure 8

Effects of aromatase inhibition on hypoxia and Su/Hx-induced changes in BMPR2 expression. **A-C: hypoxic mice**. (**A**) Relative gene expression levels of BMPR2 in male and female normoxic and hypoxic mouse lung treated with or without anastrozole 3 $mgkg^{-1}day^{-1}$ (n=6 per group). Representative immunoblot and quantification showing effects of anastrozole 3 $mgkg^{-1}day^{-1}$ on BMPR2 protein expression in (**B**) female and (**C**) male normoxic and hypoxic mouse lung (n=6 per group). **D-F: Su/Hx rats.** (**D**) Relative gene expression levels of BMPR2 in female and male normoxic and Su/Hx rat lung treated with or without anastrozole 3 $mgkg^{-1}day^{-1}$ for 14 days (n=5-6 per group). Representative immunoblot and quantification showing effects of anastrozole 3 $mgkg^{-1}day^{-1}$ on BMPR2 protein expression in (**E**) female and (**F**) male lung from normoxic and Su/Hx rats treated with or without anastrozole 3 $mgkg^{-1}day^{-1}$ for 14 days (n=5-6 per group). Gene expression levels are normalised to ² -2-microglobulin (² 2M). Data displayed as mean ± SEM. *p<0.05 and **p<0.01 as indicated, determined by one-way ANOVA with Bonferroni post test.

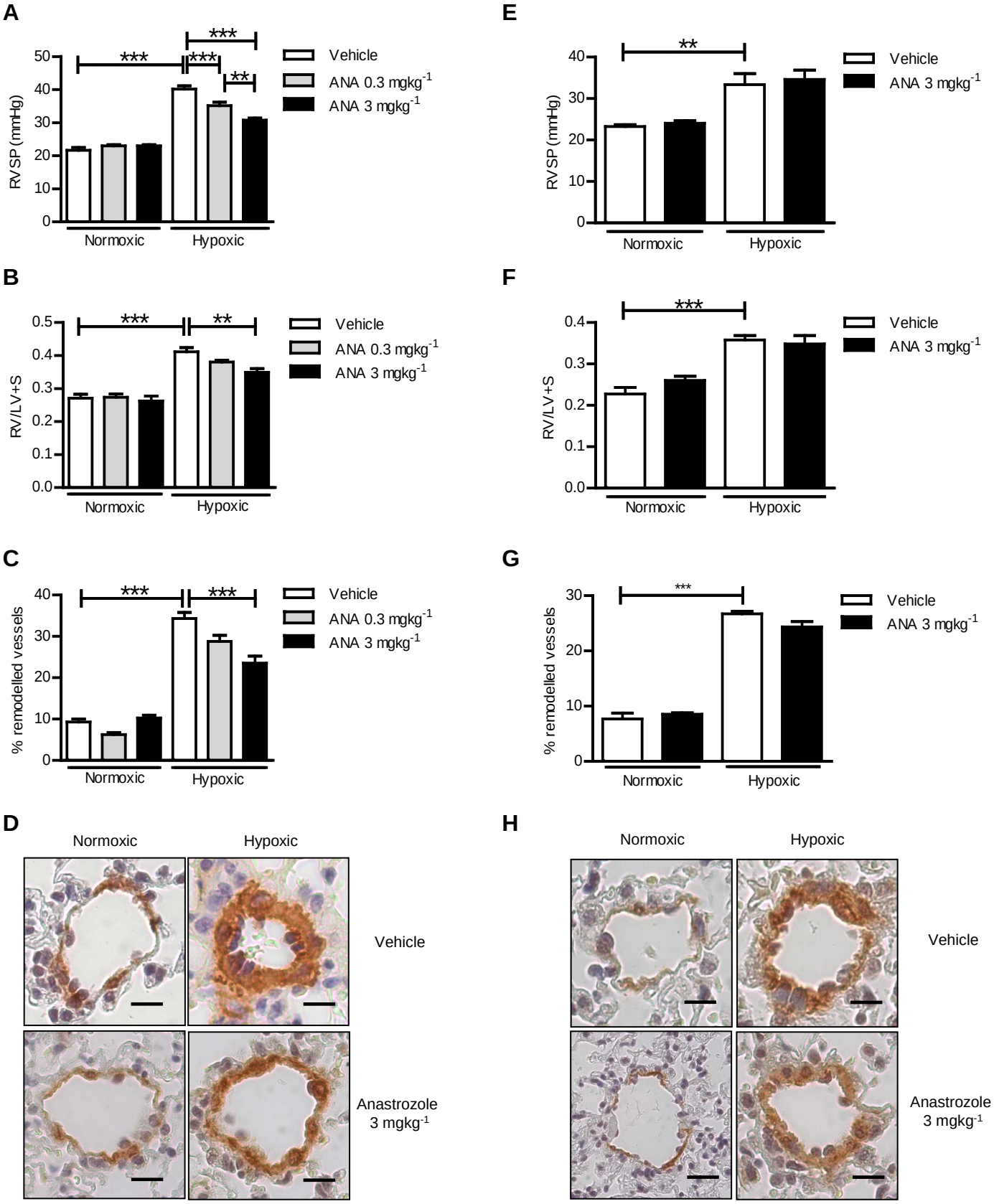
A
RVSP (mmHg)
Vehicle
ANA 0.3 mgkg-1
ANA 3 mgkg-1
Normoxic
Hypoxic
B
RV/LV+S
C
% remodelled vessels
D
E
F
G
H

Figure 1

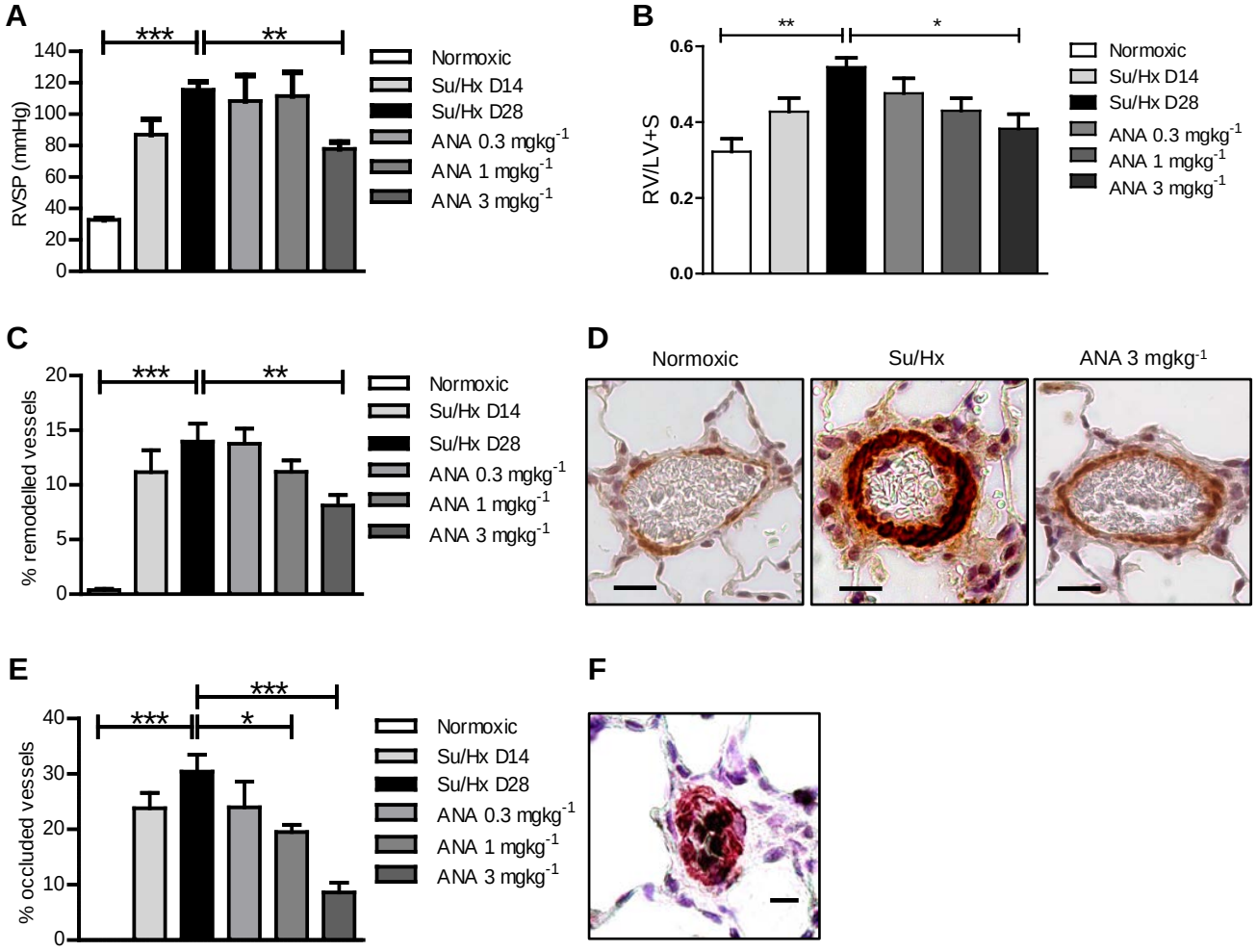
A
RVSP (mmHg)
140
120
100
80
60
40
20
0
***
**
Normoxic
Su/Hx D14
Su/Hx D28
ANA 0.3 mgkg-1
ANA 1 mgkg-1
ANA 3 mgkg-1
B
RV/LV+S
0.6
0.4
0.2
0.0
**
*
Normoxic
Su/Hx D14
Su/Hx D28
ANA 0.3 mgkg-1
ANA 1 mgkg-1
ANA 3 mgkg-1
C
% remodelled vessels
20
15
10
5
0
***
**
Normoxic
Su/Hx D14
Su/Hx D28
ANA 0.3 mgkg-1
ANA 1 mgkg-1
ANA 3 mgkg-1
D
Normoxic
Su/Hx
ANA 3 mgkg-1
E
% occluded vessels
40
30
20
10
0
***
***
*
Normoxic
Su/Hx D14
Su/Hx D28
ANA 0.3 mgkg-1
ANA 1 mgkg-1
ANA 3 mgkg-1
F

Figure 2

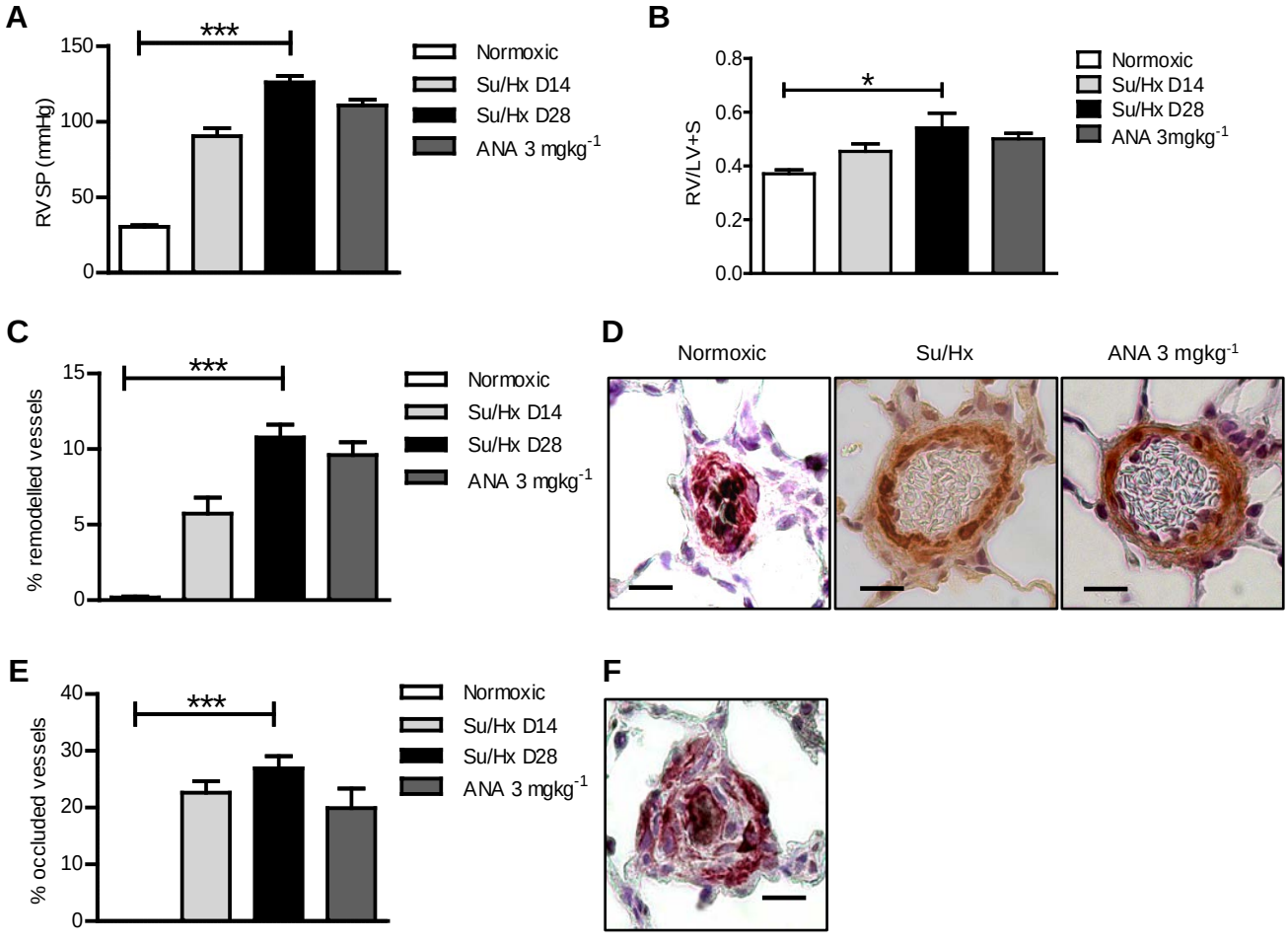
A
***
150
100
50
0
RVSP (mmHg)
Normoxic
Su/Hx D14
Su/Hx D28
ANA 3 mgkg-1
B
*
0.8
0.6
0.4
0.2
0.0
RV/LV+S
Normoxic
Su/Hx D14
Su/Hx D28
ANA 3mgkg-1
C
***
15
10
5
0
% remodelled vessels
Normoxic
Su/Hx D14
Su/Hx D28
ANA 3 mgkg-1
D
Normoxic
Su/Hx
ANA 3 mgkg-1
E
***
40
30
20
10
0
% occluded vessels
Normoxic
Su/Hx D14
Su/Hx D28
ANA 3 mgkg-1
F

Figure 3

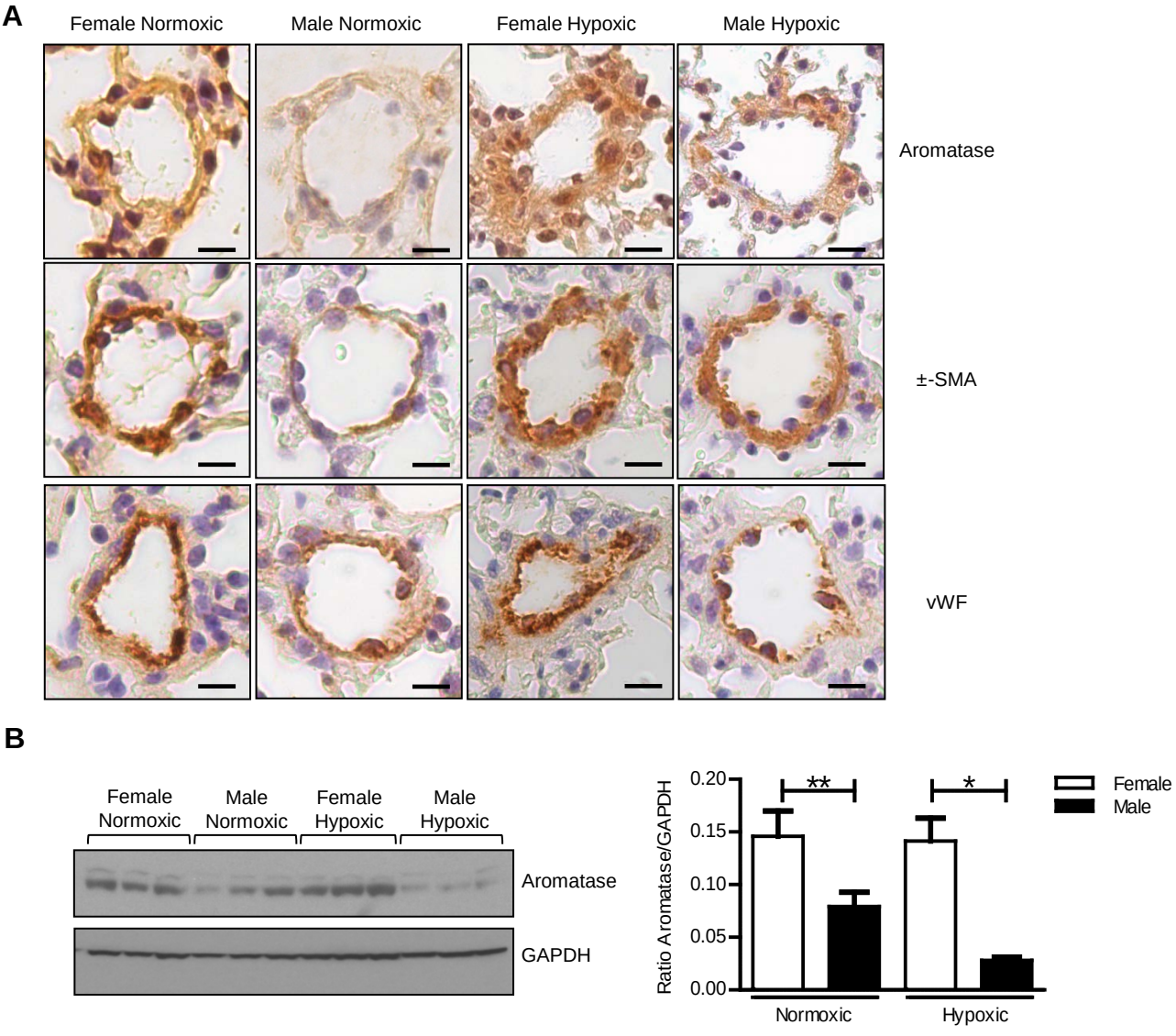
A
Female Normoxic
Male Normoxic
Female Hypoxic
Male Hypoxic
Aromatase
±-SMA
vWF
B
Female Normoxic
Male Normoxic
Female Hypoxic
Male Hypoxic
Aromatase
GAPDH
Ratio Aromatase/GAPDH
0.20
0.15
0.10
0.05
0.00
**
*
Normoxic
Hypoxic
Female
Male

Figure 4

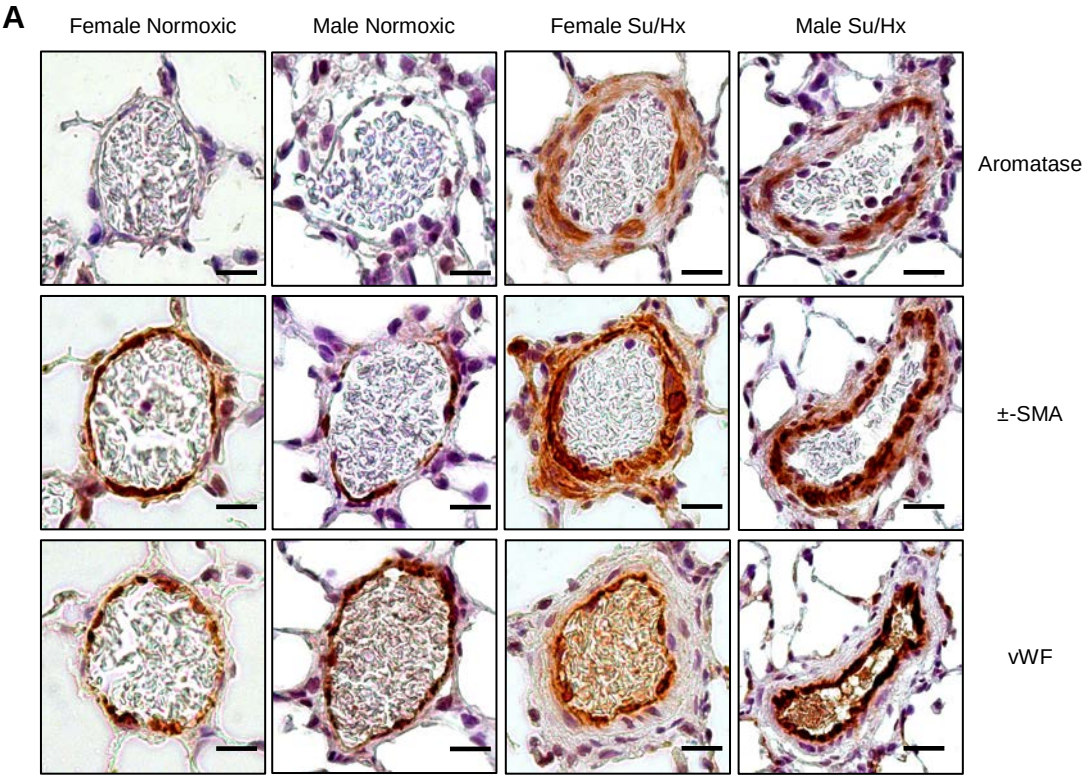
A
Female Normoxic
Male Normoxic
Female Su/Hx
Male Su/Hx
Aromatase
±-SMA
vWF

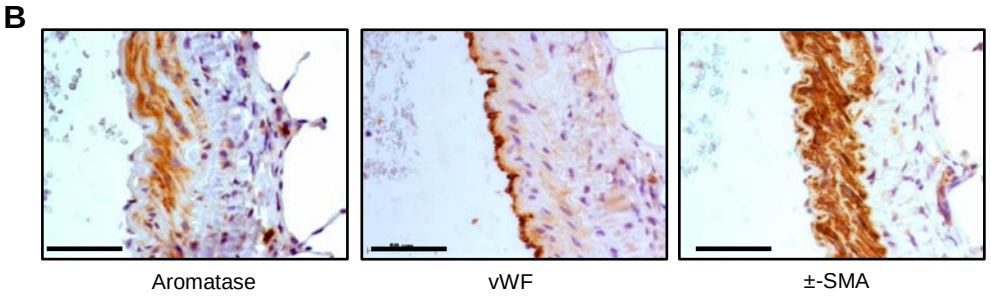
B
Aromatase
vWF
±-SMA

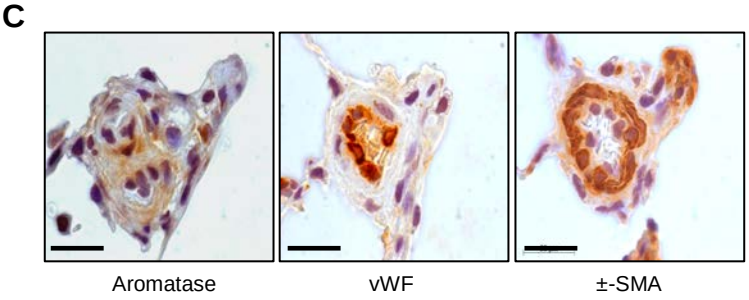
C
Aromatase
vWF
±-SMA

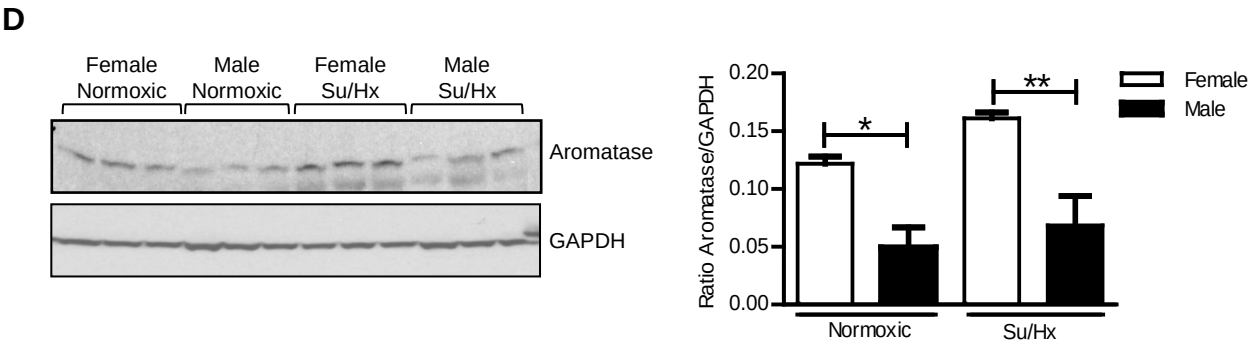
D
Female Normoxic
Male Normoxic
Female Su/Hx
Male Su/Hx
Aromatase
GAPDH
Ratio Aromatase/GAPDH
0.20
0.15
0.10
0.05
0.00
*
**
Normoxic
Su/Hx
Female
Male

Figure 5

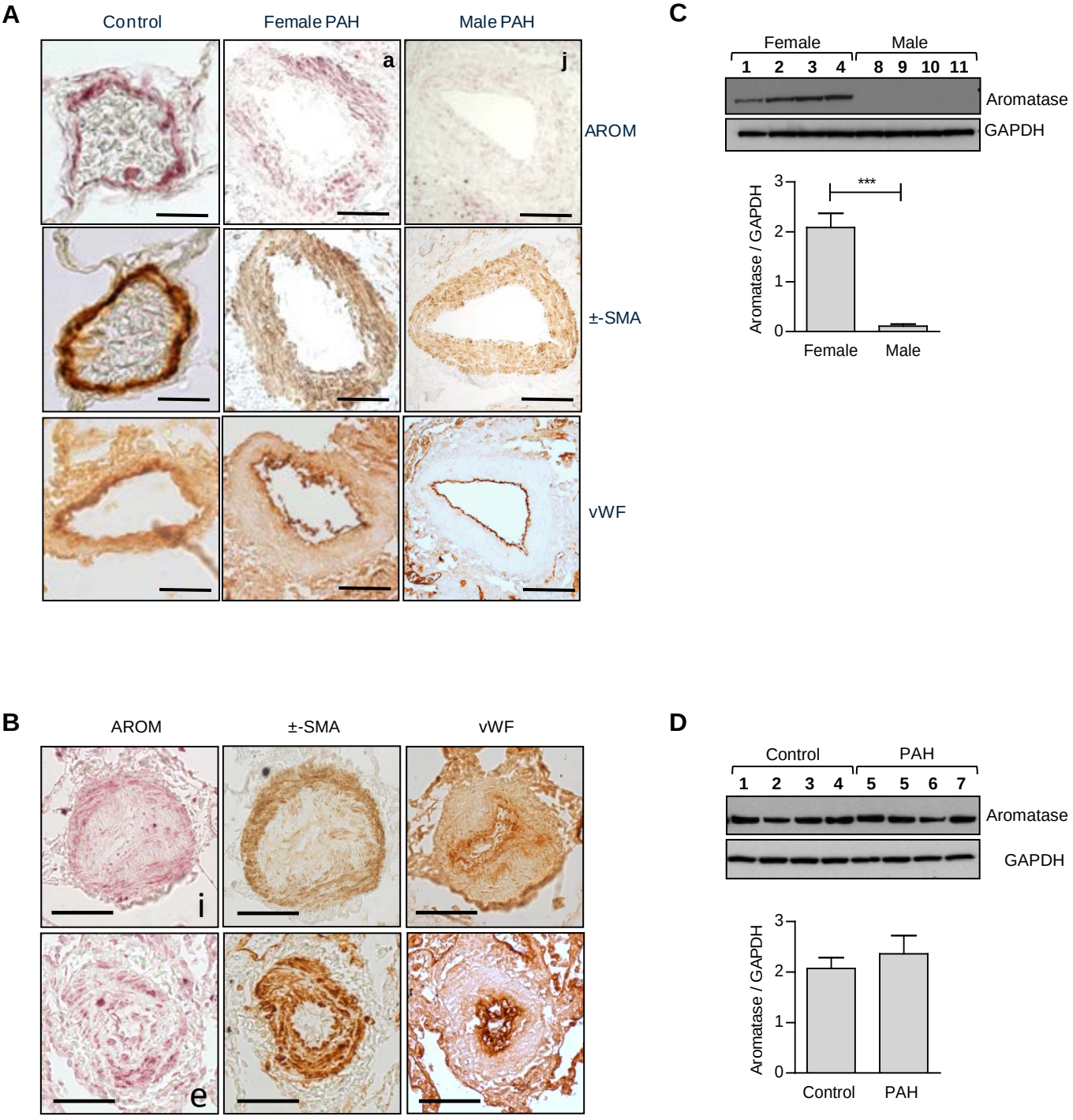
A
Control
Female PAH
Male PAH
a
j
AROM
±-SMA
vWF
B
AROM
±-SMA
vWF
i
e
C
Female
Male
1 2 3 4 8 9 10 11
Aromatase
GAPDH
***
Aromatase / GAPDH
3
2
1
0
Female
Male
D
Control
PAH
1 2 3 4 5 5 6 7
Aromatase
GAPDH
Aromatase / GAPDH
3
2
1
0
Control
PAH

Figure 6

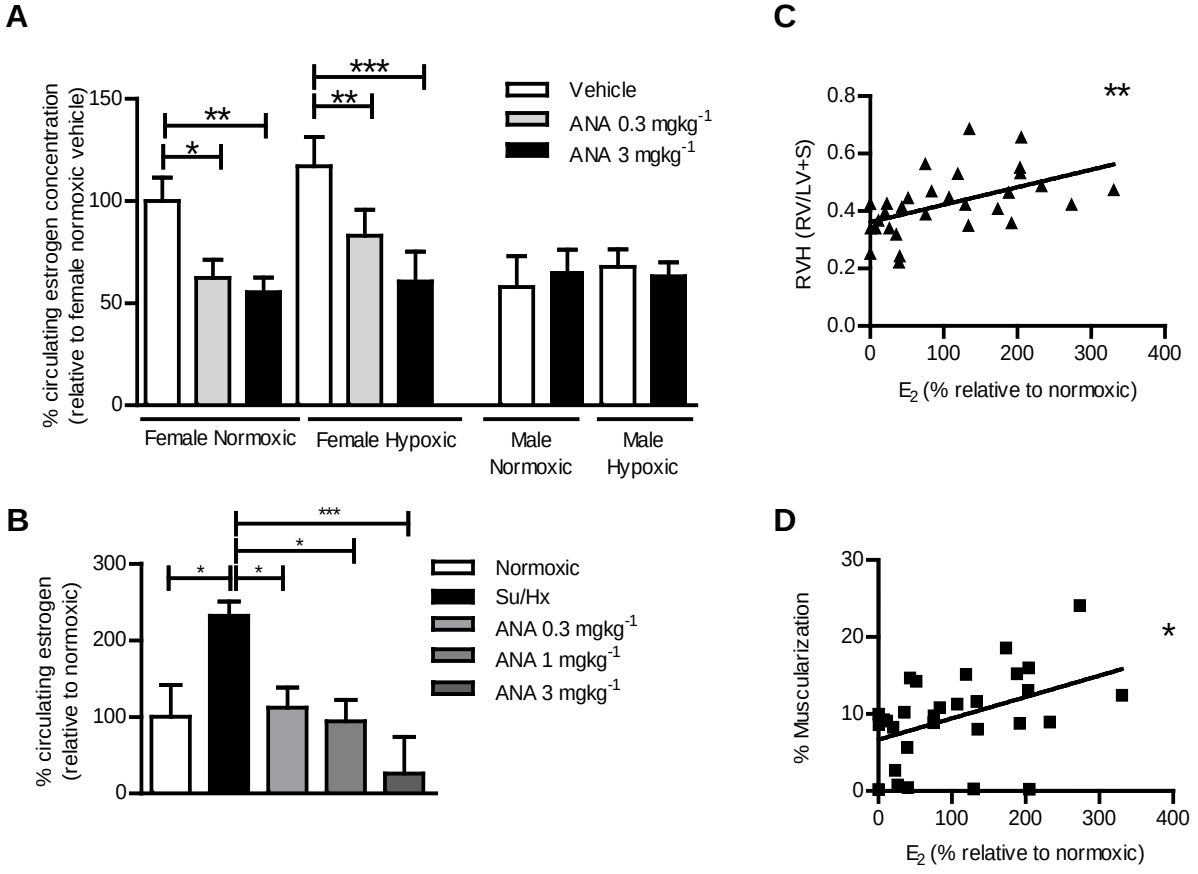
A
% circulating estrogen concentration (relative to female normoxic vehicle)
150
100
50
0
*
**
**
***
Vehicle
ANA 0.3 mgkg-1
ANA 3 mgkg-1
Female Normoxic
Female Hypoxic
Male Normoxic
Male Hypoxic
C
RVH (RV/LV+S)
0.8
0.6
0.4
0.2
0.0
**
0
100
200
300
400
E2 (% relative to normoxic)
B
% circulating estrogen (relative to normoxic)
300
200
100
0
*
*
*
***
Normoxic
Su/Hx
ANA 0.3 mgkg-1
ANA 1 mgkg-1
ANA 3 mgkg-1
D
% Muscularization
30
20
10
0
*
0
100
200
300
400
E2 (% relative to normoxic)

Figure 7

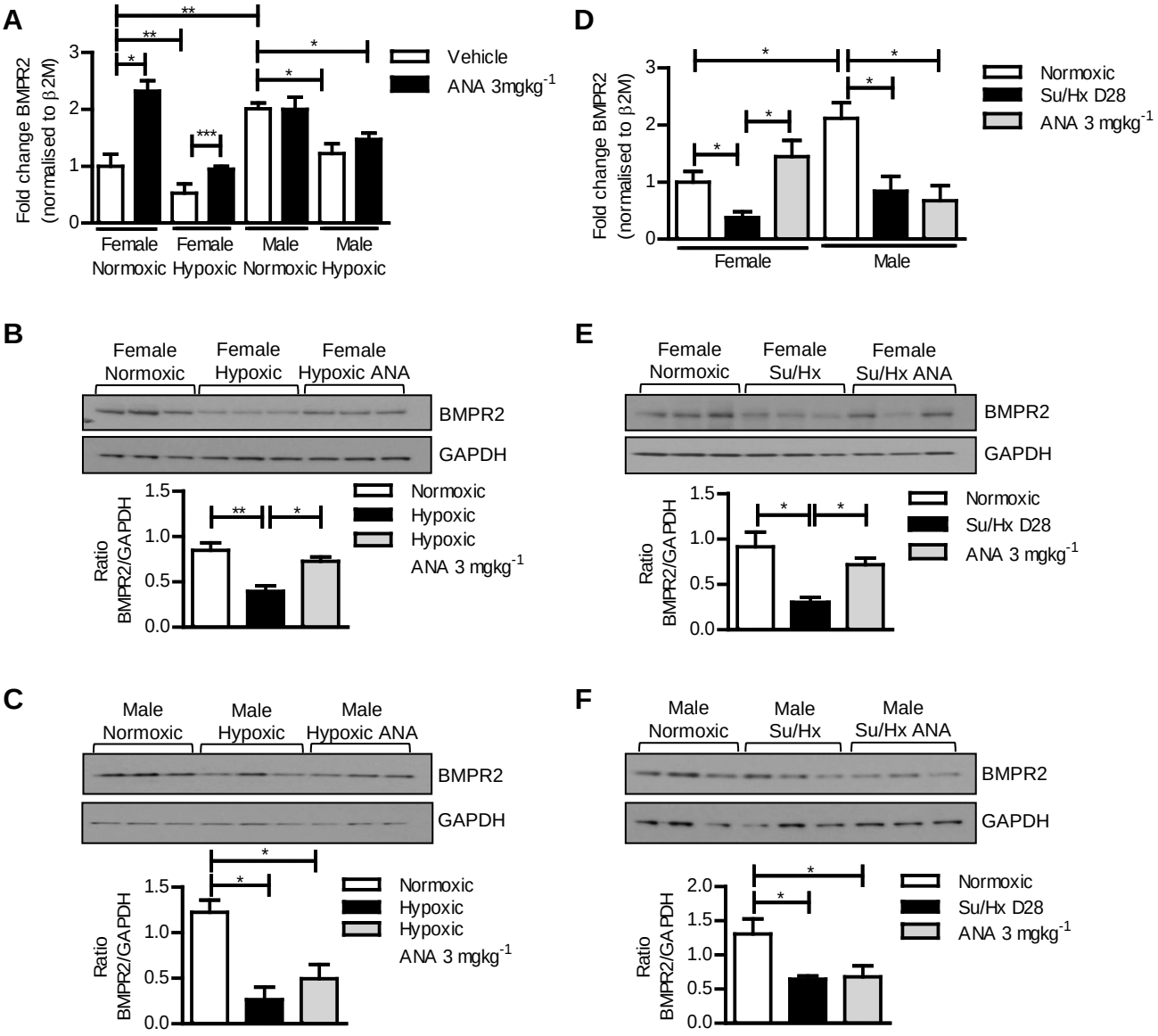
A
Fold change BMPR2 (normalised to β2M)
Vehicle
ANA 3mgkg-1
Female Normoxic
Female Hypoxic
Male Normoxic
Male Hypoxic
D
Normoxic
Su/Hx D28
ANA 3 mgkg-1
Female
Male
B
Female Normoxic
Female Hypoxic
Female Hypoxic ANA
BMPR2
GAPDH
Ratio BMPR2/GAPDH
Normoxic
Hypoxic
Hypoxic ANA 3 mgkg-1
E
Female Normoxic
Female Su/Hx
Female Su/Hx ANA
C
Male Normoxic
Male Hypoxic
Male Hypoxic ANA
F
Male Normoxic
Male Su/Hx
Male Su/Hx ANA

Figure 8

Online Data Supplement

Gender–dependent Influence of Endogenous Estrogen in Pulmonary Hypertension.

Kirsty M. Mair, Audrey F Wright, Nicholas Duggan, David J. Rowlands, Martin J. Hussey, Sonia Roberts, Josephine Fullerton, Margaret Nilsen, Lynn Loughlin, Matthew Thomas & Margaret R. MacLean.

Supplemental Methods

Ethical Information

All animal procedures conform to the UK Animal Procedures Act (1986) and the *Guide for the Care and Use of Laboratory Animals* published by the US National Institutes of Health (NIH publication No. 85–23, revised 1996). Experimental procedures using human lung tissue and hPASMCs conform to the principles outlined in the Declaration of Helsinki and were approved by Cambridgeshire 1 Research Ethics committee (REC reference: 08/H0304/56). All non-PAH human lung biopsies were confirmed as macroscopically normal and collected from patients undergoing pneumonectomy with no reported presence of PAH.

Animals

Male and female C57BL/6 mice (aged 8-12 weeks) and Wistar Kyoto rats (~200g) were purchased from Harlan, UK. Rodents were housed in a 12-hour light-dark cycle with access to food and water ad libitum. Animals were housed together to promote synchronisation of the estrous cycle. The method we employ to check the estrous cycle in cohorts of mice is as follows. All female mice are housed together for two weeks prior to the study. A blunt, shortened tip of a Pasteur pipette is placed at the vaginal orifice. One drop of PBS is gently expelled into the vagina and aspirated back before being transferred to a microscope slide. Smears are examined microscopically and classified as to the stage of the cycle according to criteria modified from those of Nelson *et al.,* (1). Our analysis indicates that even after 4 days female mice start to synchronise and by two weeks we are convinced that they

are fully synchronised. In addition, plasma levels of estrogen are very consistent and within a tight range for our female study animals.

In Vivo Effects of MPP Dihydrochloride Administration

Prior to the induction of hypoxia, C57Bl/6 mice were administered with either ER± antagonist, MPP dihydrochloride [chemical name- 1,3-Bis(4-hydroxyphenyl)-4-methyl-5-[4-(2-piperidinylethoxy)phenol]-1H-pyrazole dihydrochloride] (MPP) 2 $mgkg^{-1}day^{-1}$ or vehicle. Under general anaesthesia (1% - 3% (v/v) isoflurane supplemented with O_2) pellets containing either ER± antagonist, MPP (0.56mg/14 day pellet, Innovative Research of America, Florida, USA) or vehicle were inserted subcutaneously into the dorsal neck of male and ovary intact female mice using a sterile 12-gauge hypodermic needle. The development of PH was then assessed in normoxic animals and animals exposed to hypobaric hypoxia (550mbar, equivalent to 10% O_2) for 14 days in the presence of MPP or vehicle. n=6-10 mice per experimental group.

Sugen 5416+hypoxia

The underlying concept is that two hits are required to generate severe obliterative PH in the rat. Su5416 binds with high affinity to the intracellular tyrosine kinase domain of VEGFR1 (flt1) and VEGFR2 (KDR) and inhibits signal transduction via these receptors, inducing lung endothelial cell apoptosis (2). Su5416-induced pulmonary endothelial cell apoptosis in combination with chronic hypoxia results in the development of angioproliferation and obliterative pulmonary vascular lesions (3).

The vascular endothelial growth factor receptor inhibitor Sugen (Su) 5416 was suspended in 0.5% (wt/vol) carboxymethylcellulose sodium, 0.9% (wt/vol) NaCl, 0.4% (vol/vol) polysorbate, and 0.9% (vol/vol) benzyl alcohol in dH2O. Rats (~200g) were administered with a single injection of Su5416 (Sigma UK, 20 $mgkg^{-1}$ s.c.) or 0.9% saline and exposed to chronic hypoxia for 14 days. At this point, a sub-set of animals were taken for hemodynamic and histological analysis. The remaining rats were subsequently transferred to normoxic conditions for a further 14 days during which time the received the aromatase inhibitor anastrozole 0.03, 0.3 or 3 $mgkg^{-1}day^{-1}$ or vehicle (1% carboxymethylcellulose) by oral administration. Vehicle dosed rats housed in normoxic conditions only were studied as controls.

Echocardiographic Assessment and pressure measurements in rats

In rats, right ventricular systolic pressure was measured by right heart catheterization through the right jugular vein (MPVS-300 System; Millar, Houston, TX).

Echocardiographic assessments were performed by ultrasound on 2% isoflurane-anesthetized animals. A Vivid7 (GE Healthcare, Little Chalfont, Buckinghamshire, UK) ultrasound system equipped with 13-MHz probe was used. The pediatric probe was placed in a parasternal long axis position to visualize the PA outflow tract. Pulsed flow Doppler imaging was then overlaid to observe the dynamics of blood flow through the PA valve. Changes in PA acceleration/ejection time ratio (time taken from start of flow to maximal velocity or to the end of flow) were determined. The cardiac function was further analyzed by cardiac output (CO) values as previously described (4). Analysis was performed using Echo-PAC dimension software.

Right Ventricular Hypertrophy

Right ventricular hypertrophy (RVH) in mice was assessed by weight measurement of the right ventricular free wall and left ventricle plus septum. The ratio expressed is RV/LV+S.

Lung Histopathology

3µm lung sagittal sections were stained with elastic Van Gieson and pulmonary arteries (<80 µm external diameter) microscopically assessed for degree of muscularisation in a blinded fashion, as previously described (5). Remodelled arteries were confirmed by the presence of double-elastic laminae. Briefly, percentage remodelling (percent of remodelled vessels) was defined for each animal by the number of remodelled vessels divided by the total number (e80 per lung) of vessels observed in the lung. To visualize the degree of smooth muscle thickening, lungs were stained with ±-smooth muscle actin (Abcam, UK). Briefly, 3 µm sagittal sections were deparaffinised and rehydrated through a xylene-ethanol gradient. After epitope retrieval, endogenous peroxidase and biotin activity was blocked and lung tissue was incubated for 16 hours with anti-rabbit ±-smooth muscle actin antibody (dilution 1:1000 Abcam, UK) or IgG control. After secondary incubation, ±-smooth muscle actin was visualized with the DAB substrate kit (Vector Laboratories, UK), which stained brown/dark brown. The presence and degree of pulmonary vascular occlusion formation were assessed in lungs from chronic hypoxic+SU5416–treated rats as previously described (5). Images were captured using a Zeiss Axio Imager M1.

Quantitative Reverse Transcription–Polymerase Chain Reaction

mRNA expression was assessed in the lungs of mice by quantitative reverse transcription–polymerase chain reaction. At necropsy, lung tissue from each rodent was removed and snap frozen. RNA was then extracted from the lung tissue or pulmonary artery smooth muscle cells and gene expression quantified using TaqMan® gene expression assays (assay details shown in Supplemental Table 1). ViiA7 Real-time PCR system (Applied Biosystems) was programmed for PCR conditions 95oC for 10 minutes followed by 50 cycles of 95^{o}C for 15 seconds and 60^{o}C for 1 minute. Results were normalised to ² -2-microglobulin. The fold change for every gene was obtained using the $2^{-" " Ct}$ method and expressed relative to normoxic female mice or rats as appropriate.

Immunoblotting

Protein expression was assessed in whole lung. Briefly, lung tissue was homogenised in radioimmunoprecipitation assay buffer via ultrasonic homogenization. Samples were denatured and electrophoresed on SDS-PAGE gel. 30µg protein for each sample was loaded per well. Separated proteins were transferred to PVDF membrane and incubated for 1 hour with 5% milk/TBST (w/v) before incubating overnight at 4^{o}C with antibodies against aromatase, TPH-1, BMPR2 and GAPDH (for details of primary antibodies used refer to Supplemental Table 2). Aromatase, TPH-1, BMPR2 and GAPDH molecular weights were detected at 55, 51, 115 and 37 kDa, respectively. Densitometric analysis was performed with TotalLab TL100 software. Data are expressed relative to GAPDH density.

Lung Immunolocalization

Pulmonary vascular aromatase expression was investigated in murine, rat and human lung by immunohistochemistry. Briefly, 5 µm sagittal sections were deparaffinised and rehydrated through a xylene-ethanol gradient. After epitope retrieval, endogenous peroxidase and biotin activity was blocked and lung tissue was incubated for 16 hours with anti-rabbit aromatase antibody or IgG control. 5µm consecutive sections were also incubated with ±-smooth muscle actin (±-SMA) and von Willebrands factor (vWF) to determine aromatase localisation within the vessel wall. After secondary incubation, aromatase, ±-SMA and vWF were visualized with the DAB substrate kit (Vector Laboratories, UK), which stained brown/dark brown. In the case of human lung tissue aromatase was visualized with the VIP substrate kit (Vector Laboratories, UK), which stained pink. Images were captured using a Zeiss Axio Imager M1. For details of primary antibodies used refer to Supplemental Table 2.

Human microvascular pulmonary artery endothelial cells (hMPAECs)

(hMPAECs) were grown from surgically discarded lung tissues collected from donors that underwent pulmonary resection for reasons not related to PH (female, 42 year old caucausian) (PromoCell). Cultured PAECs were grown in Endothelial Cell Growth Medium 2 (EGM-2; PromoCell) and utilized for experimental analysis from passage 3–6 inclusive.

hPASMCs and PAH-PASMCs

hPASMCs were provided by Professor N.W. Morrell (University of Cambridge, Cambridge, UK). Briefly, hPASMCs were explanted from the distal pulmonary

arteries of macroscopically normal lung tissue at transplantation, with the patient having no reported presence of PAH. PAH-PASMCs were explanted from the distal pulmonary arteries of patients diagnosed with PAH immediately after pneumonectomy. The hPASMCs were isolated from peripheral segments of artery (0.3 to 1.0mm external diameter) by microdissection, as previously described (6). For experiments PASMCs were plated in 10% FBS/DMEM and used between passages 5 to 8. Cultured hPASMCs were confirmed by both staining for ±-smooth muscle actin (>97% ±-smooth muscle actin–positive cells) and morphological characterization (6). Table E3 describes the clinical characteristics of the human cells and tissues studied.

Figure E1

Systemic arterial blood pressure and heart rate in chronic hypoxic mice model treated with anastrozole. Effects of the aromatase inhibitor, anastrozole (ANA) 0.3 $mg^{-1}kg^{-1}day^{-1}$ and 3 $mgkg^{-1}day^{-1}$ for 14 days on (**A**) systemic arterial pressure(mSAP) (n=7-9 per group) and (**B**) heart rate (HR) in female mice (n=7-9 per group); and effects of anastrozole 3 $mgkg^{-1}day^{-1}$ for 14 days on (**D**) mSAP (n=6 per group) and (**E**) HR in male mice (n=6 per group). Data displayed as mean ± SEM, analysed by one-way ANOVA with Bonferroni post test.

Figure E2

Estrogen receptor expression is altered in female mouse pulmonary artery in hypoxia. **Female mice:** (A) ER± protein expression and (B) ER^2 protein expression in normoxic and hypoxic pulmonary arteries from female mice. **Male mice:** (A) ER± protein expression and (B) ER^2 protein expression in normoxic and hypoxic pulmonary arteries from male mice. Representative immunoblots and graph showing quantification comparing ER± and ER^2 expression for n=3 pulmonary arteries per group. Data are shown as mean ± SEM and analysed using an unpaired t-test. *$p<0.05$ vs. Normoxic

Figure E3

MPP 2mgkg^{-1}day^{-1} attenuates the development of hypoxic pulmonary hypertension in female mice whilst male mice are unaffected**. A-D: female mice.** Right ventricular systolic pressure (RVSP) (A), right ventricular hypertrophy (RV/LV+S) (B) and pulmonary vascular remodelling (C&D) assessment in female mice. **E-H: male mice.** RVSP (E), RV/LV+S (F) and pulmonary vascular remodelling (G&H) are unaffected in males. Representative images of distal pulmonary arteries from each group are shown, (alpha-SMA stains dark brown). Data are expressed as ± SEM analysed by two-way ANOVA followed by a Bonferroni post-hoc test. * $p<0.05$; ** $p<0.01$; *** $p<0.001$ vs. normoxic; † $p<0.05$ vs. vehicle. n=6-9 per group. Scale bar (**-**)=20µm.

Figure E4

Effect of aromatase inhibition on cardiac function the female and male Su5416/hypoxia(Su/Hx) rats. (**A**) Cardiac output as determined by echocardiogram on day 14 (D14) and day 28 (D28) following administration of Su/Hx in female rats treated with or without anastrozole (ANA) 0.03 $mgkg^{-1}day^{-1}$, 0.3 $mgkg^{-1}day^{-1}$ or 3 $mgkg^{-1}day^{-1}$ in female rats (n=4-5 per group) and (**B**) Pulmonary artery acceleration time measured serially by echocardiogram at days 0, 14 and 28 in female Su/Hx rats treated with or without anastrozole (n=5 per group). Cardiac parameters were also studied in male Su/Hx rats. (**C**) Cardiac output as determined by echocardiogram on day 14 (D14) and day 28 (D28) following administration of Su/Hx in male rats treated with or without anastrozole 3 $mgkg^{-1}day^{-1}$ (n=5 per group) and (**D**) Pulmonary artery acceleration time at days 0, 14 and 28 in male SUGEN/hypoxic rats treated with or without anastrozole (n=5 per group). Data displayed as mean ± SEM. **p<0.01 as indicated, determined by one-way ANOVA with Dunnett's post test.

Figure E5

Examples of aromatase immunoreactivity in human lung and human microvascular pulmonary artery endothelial cells (hMPAECs). (A) Representative image of IgG controls in mouse, rat and human pulmonary artery. (B) Representative images showing aromatase immunolocalisation in a pulmonary artery from a female PAH patient (aromatase = pink; ±-smooth muscle actin (±-SMA) = brown; von Willebrand factor (vWF) = brown; scale bar (-) indicates 500µm). **b** corresponds to patient information in Supplemental Table E3. (C) Immunoblot showing absence of aromatase expression in hMPAECs from 4 separate samples. Mouse uterus was used as a positive control for the aromatase antibody.

Figure E6

Effects of aromatase inhibition on hypoxia and Su/Hx-induced changes in Id expression. **A-B: hypoxic mice.** Relative gene expression levels in whole lung of (**A**) Id1 and (**B**) Id3 in male and female normoxic and hypoxic mice treated with or without anastrozole (ANA) 3 $mgkg^{-1}day^{-1}$ (n=6 per group). **D-F: Su/Hx rats.** (**C**) Id 1 and (**D**) Id3 relative mRNA levels in female and male normoxic and SUGEN/hypoxic rat lung treated with or without anastrozole 3 $mgkg^{-1}day^{-1}$ for 14 days (n=5-6 per group). Gene expression levels are normalised to ² -2-microglobulin (² 2M). Data displayed as mean ± SEM. *p<0.05 and **p<0.01 as indicated, determined by one-way ANOVA with Bonferroni post test.

Figure E7

Effects of ER± antagonist MPP on BMPR2 and Id1 expression in hypoxic female mice. Relative gene expression levels of **A** BMPR2 and **B** Id1 in whole lung form female normoxic and hypoxic mice treated with or without MPP 2$mgkg^{-1}day^{-1}$ (n=6 per group). Gene expression levels are normalised to GAPDH). Data displayed as mean ± SEM. *p<0.05 and **p<0.01 as indicated, determined by one-way ANOVA with Bonferroni post test.

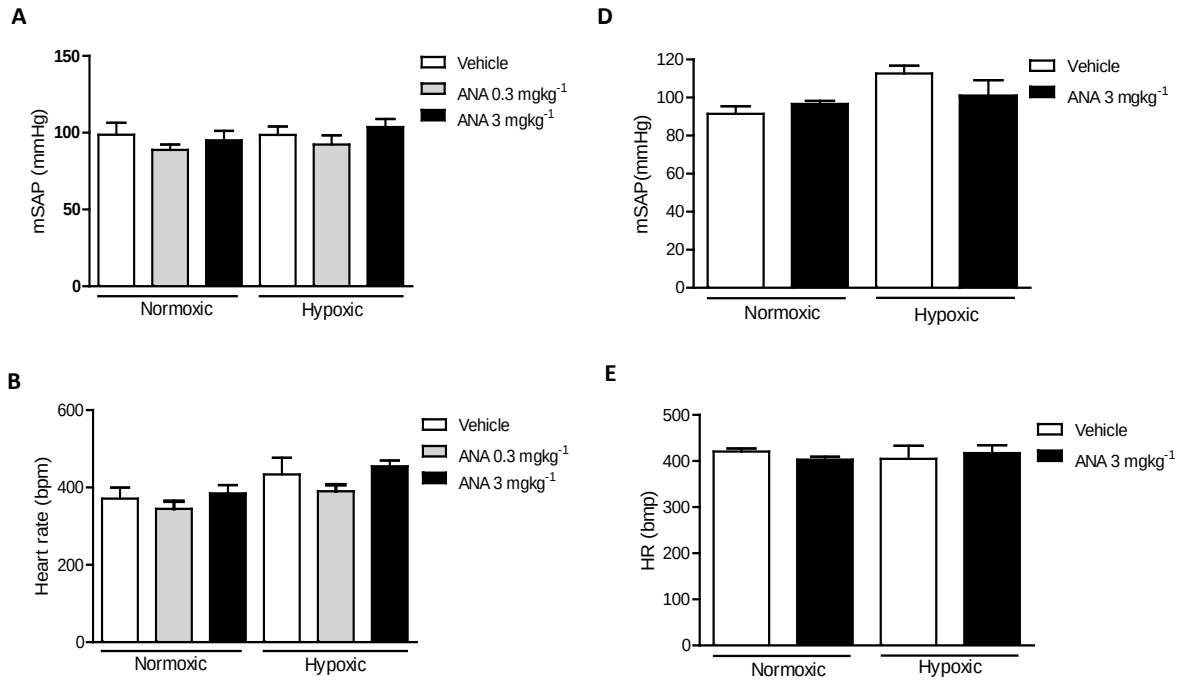
A
mSAP (mmHg)
150
100
50
0
Normoxic
Hypoxic
Vehicle
ANA 0.3 mgkg-1
ANA 3 mgkg-1
D
mSAP(mmHg)
120
100
80
60
40
20
0
Normoxic
Hypoxic
Vehicle
ANA 3 mgkg-1
B
Heart rate (bpm)
600
400
200
0
Normoxic
Hypoxic
Vehicle
ANA 0.3 mgkg-1
ANA 3 mgkg-1
E
HR (bmp)
500
400
300
200
100
0
Normoxic
Hypoxic
Vehicle
ANA 3 mgkg-1

Figure E1.

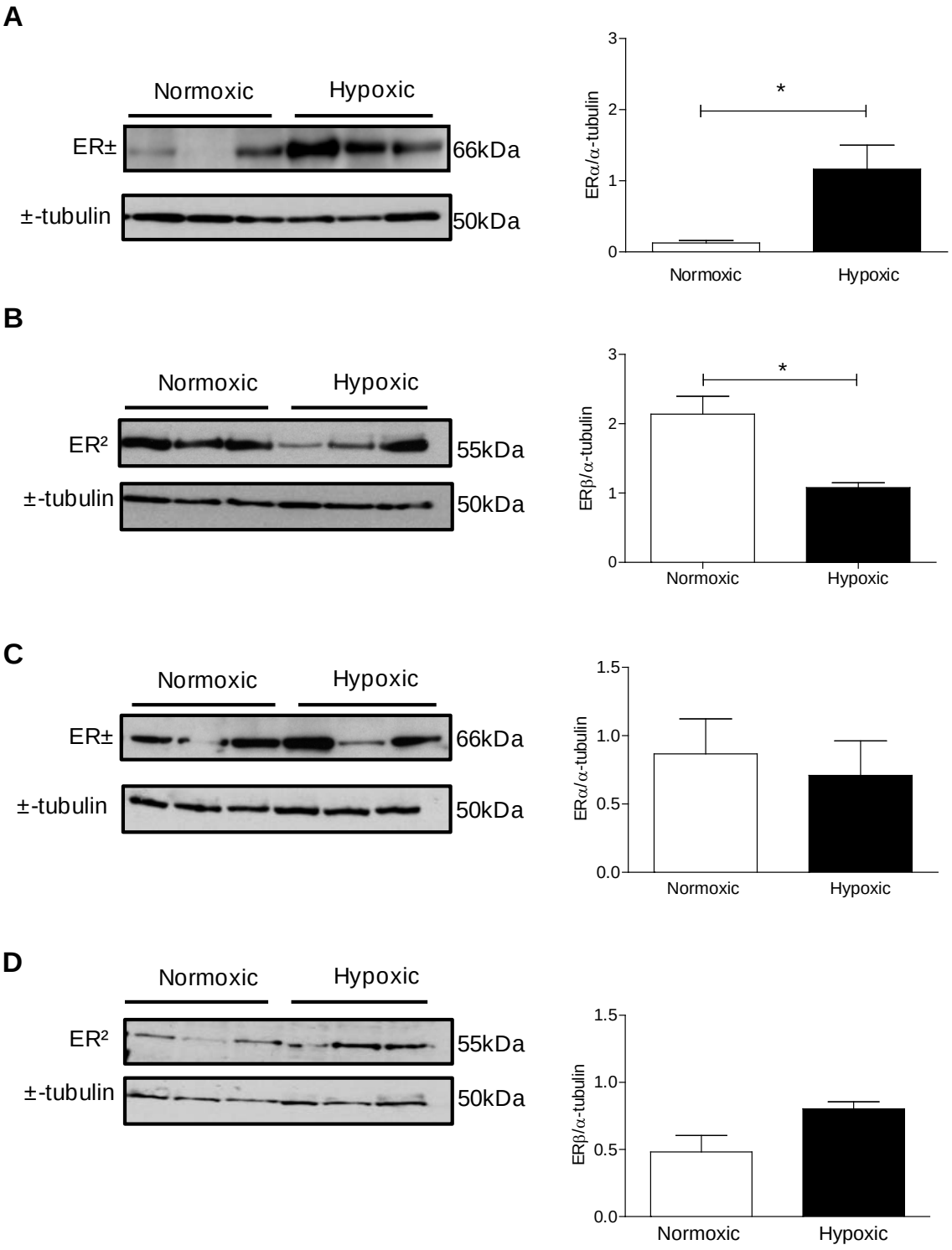
A
Normoxic
Hypoxic
ER±
66kDa
±-tubulin
50kDa
ERα/α-tubulin
3
2
1
0
*
Normoxic
Hypoxic
B
Normoxic
Hypoxic
ER²
55kDa
±-tubulin
50kDa
ERβ/α-tubulin
3
2
1
0
*
Normoxic
Hypoxic
C
Normoxic
Hypoxic
ER±
66kDa
±-tubulin
50kDa
ERα/α-tubulin
1.5
1.0
0.5
0.0
Normoxic
Hypoxic
D
Normoxic
Hypoxic
ER²
55kDa
±-tubulin
50kDa
ERβ/α-tubulin
1.5
1.0
0.5
0.0
Normoxic
Hypoxic

Figure E2

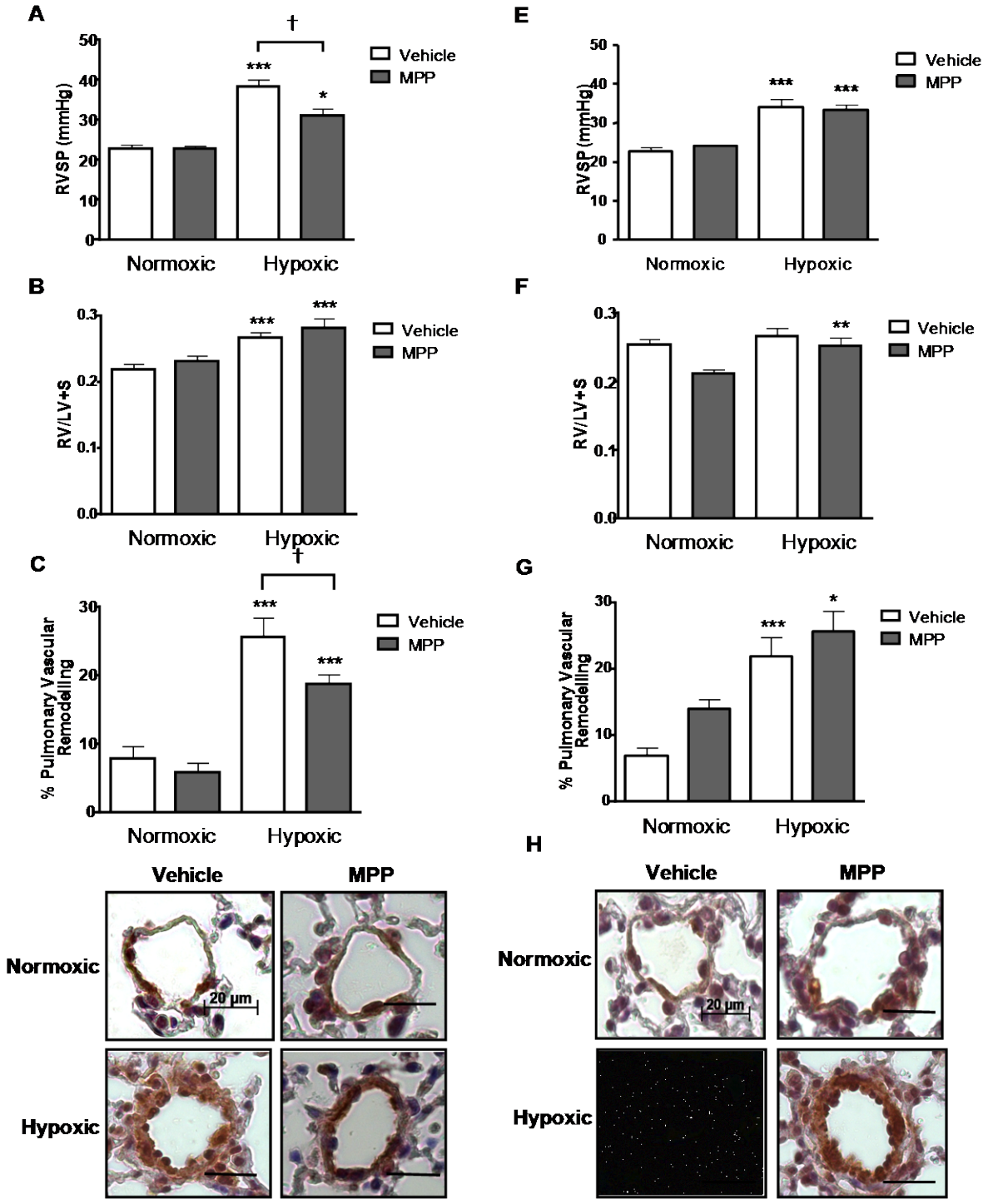
A
RVSP (mmHg)
Vehicle
MPP
Normoxic
Hypoxic
B
RV/LV+S
C
% Pulmonary Vascular Remodelling
E
F
G
H
Vehicle
MPP
Normoxic
Hypoxic
20 μm

Figure E3

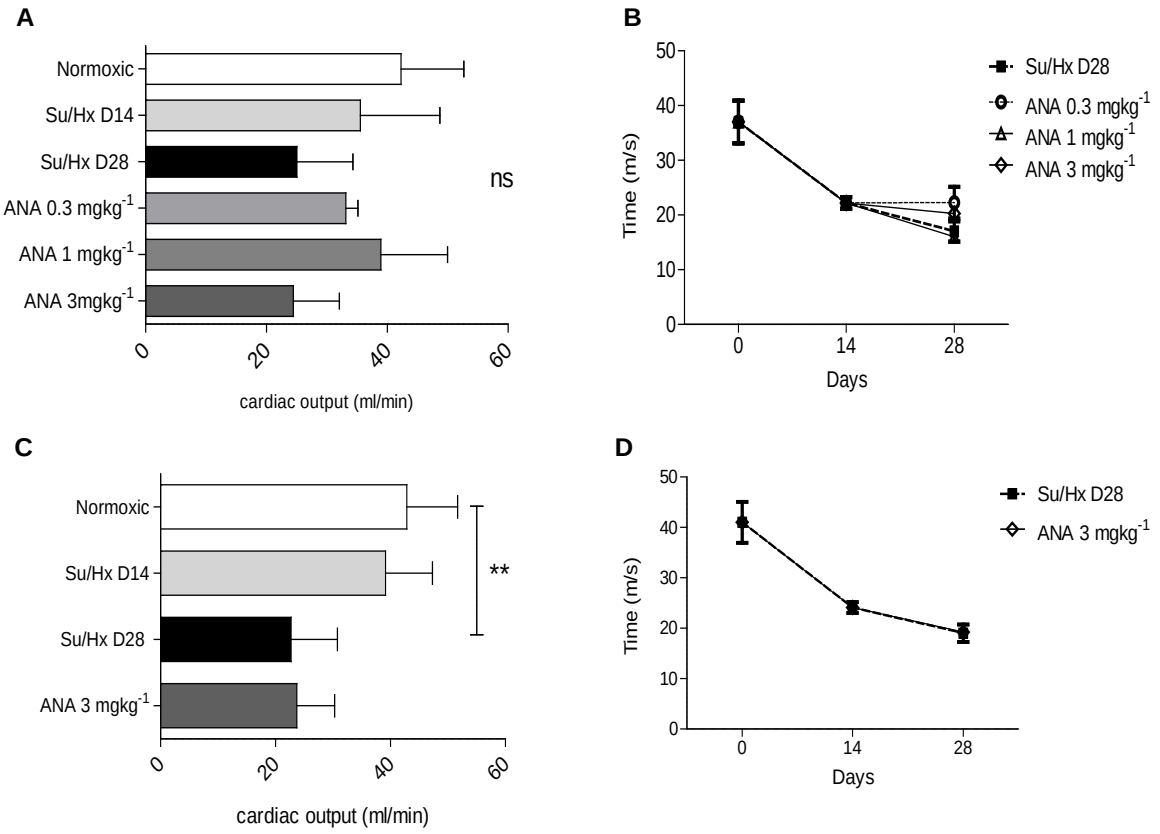
A
Normoxic
Su/Hx D14
Su/Hx D28
ANA 0.3 mgkg-1
ANA 1 mgkg-1
ANA 3mgkg-1
ns
0
20
40
60
cardiac output (ml/min)
B
Time (m/s)
Days
Su/Hx D28
ANA 0.3 mgkg-1
ANA 1 mgkg-1
ANA 3 mgkg-1
C
Normoxic
Su/Hx D14
Su/Hx D28
ANA 3 mgkg-1
**
cardiac output (ml/min)
D
Time (m/s)
Days
Su/Hx D28
ANA 3 mgkg-1

Figure E4

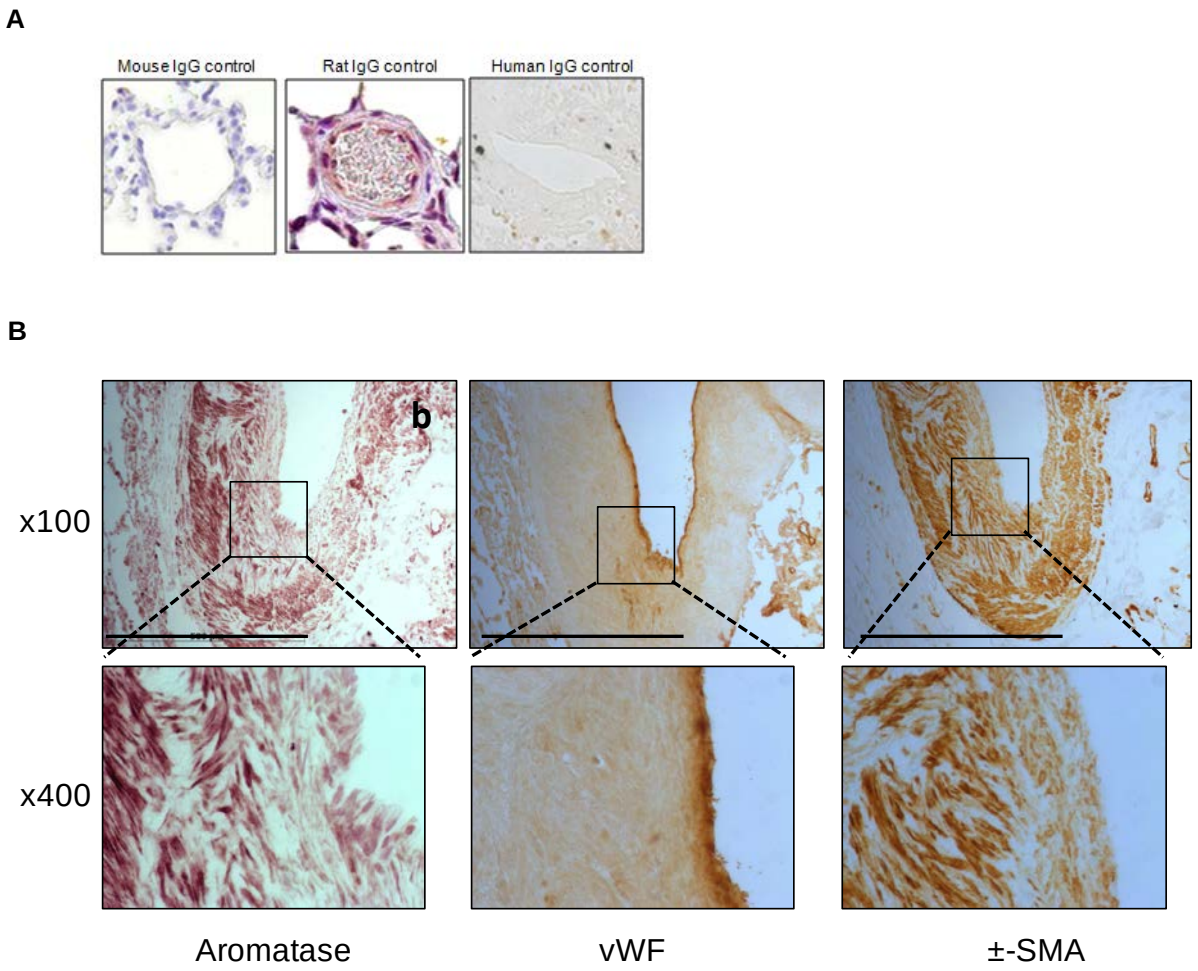
A
Mouse IgG control
Rat IgG control
Human IgG control
B
x100
x400
b
Aromatase
vWF
±-SMA
C
Human microvascular pulmonary artery endothelial cells
Uterus
Aromatase
GAPDH

Figure E5

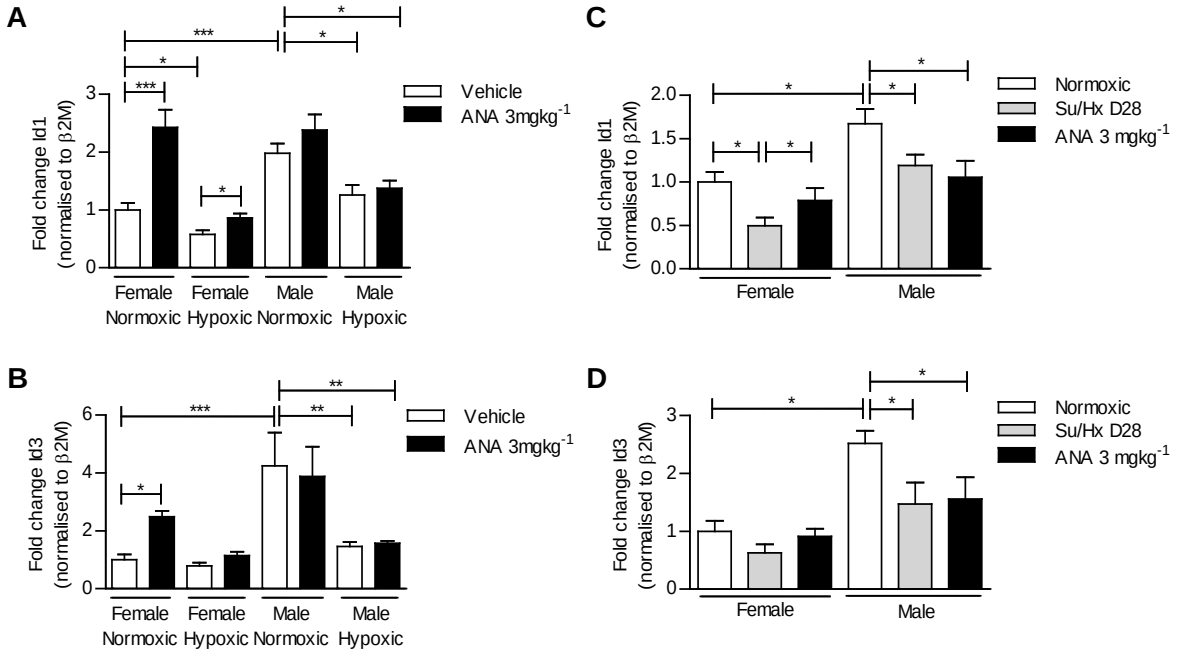
A
Fold change Id1 (normalised to β2M)
Vehicle
ANA 3mgkg-1
Female Normoxic
Female Hypoxic
Male Normoxic
Male Hypoxic
B
Fold change Id3 (normalised to β2M)
Vehicle
ANA 3mgkg-1
Female Normoxic
Female Hypoxic
Male Normoxic
Male Hypoxic
C
Fold change Id1 (normalised to β2M)
Normoxic
Su/Hx D28
ANA 3 mgkg-1
Female
Male
D
Fold change Id3 (normalised to β2M)
Normoxic
Su/Hx D28
ANA 3 mgkg-1
Female
Male

Figure E6

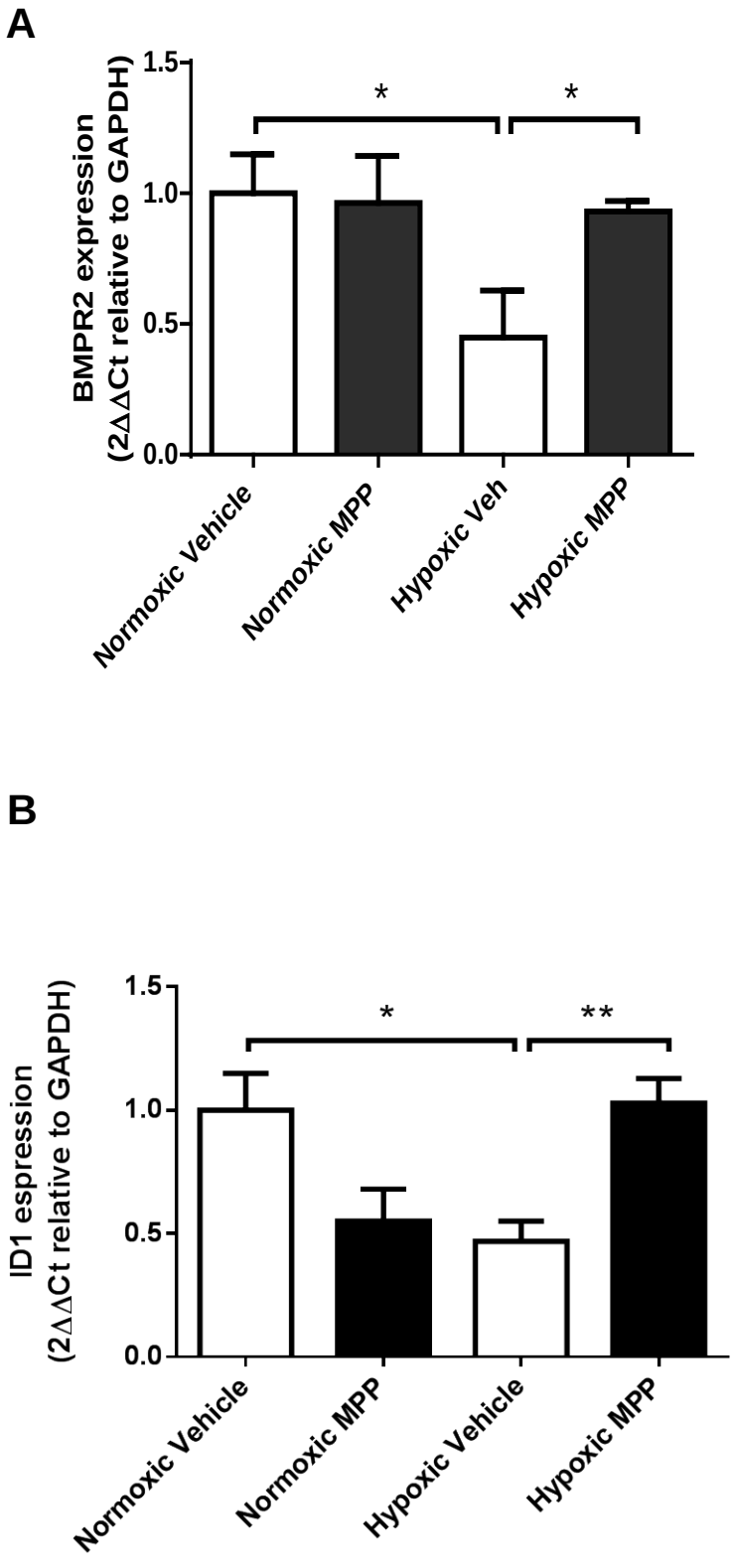
A
BMPR2 expression
(2ΔΔCt relative to GAPDH)
1.5
1.0
0.5
0.0
*
*
Normoxic Vehicle
Normoxic MPP
Hypoxic Veh
Hypoxic MPP
B
ID1 espression
(2ΔΔCt relative to GAPDH)
1.5
1.0
0.5
0.0
*
**
Normoxic Vehicle
Normoxic MPP
Hypoxic Vehicle
Hypoxic MPP

Figure E7

Gene	***Species***	***Assay ID***
BMPR2	*Mouse* *Rat*	*Mm00432134_m1* *Rn01437213_m1*
Id1	*Mouse* *Rat*	*Mm00775963_g1* *Rn00562985_s1*
Id3	*Mouse* *Rat*	*Mm01188138_g1* *Rn04219390_g1*
² -2-microglobulin	*Mouse* *Rat*	*Mm00437762_m1* *Rn00560865_m1*

Table E1. TaqMan gene expression assays purchased from Applied Biosystems.

Antibody	***Type (Clone)***	***Source (catalogue number)***	***Dilution used***
Aromatase	*Rabbit polyclonal*	*Abcam (ab69653)*	*Immunoblotting: 1:1000* *Immunohistochemistry: 1:120*
BMPR2	*Mouse monoclonal*	*BD Bioscience (612292)*	*Immunoblotting: 1:500*
GAPDH	*Mouse monoclonal [mAbcam 9484]*	*Abcam (ab9482)*	*Immunoblotting: 1:10000*
±-SMA	*Rabbit polyclonal*	*Abcam (ab5694)*	*Immunohistochemistry: 1:500*
vWF	*Rabbit polyclonal*	*Dako (A0082)*	*Immunohistochemistry: 1:1000*

Table E2. Specifications and sources of antibodies used for immunoblotting and immunohistochemistry.

±-SMA indicates ±-smooth muscle actin and vWF indicated von Williebrands factor.

	Tissue Type	***Available Patient information***	***BMPR2 mutation***
Non PAH - Female	PASMCs	**1.** 58 year old **2.** 64 year old **3.** 59 year old **4.** 64 year old	
PAH - Female	Lung	**a.** 26 year old, HPAH, transplant, meanPAP 58mmHg **b.** 30 year old HPAH, transplant, meanPAP 46mmHg **c.** 38 year old HPAH, transplant, meanPAP 56mmHg **d.** 19 year old HPAH, transplant **e.** 26 year old IPAH, transplant **f.** 44 year old IPAH, transplant **g.** 51 year old IPAH, transplant **h.** 23 year old IPAH, transplant	Yes Yes
	PASMCs	**5.** 24 year old , IPAH **6.** 39 year old, HPAH **7.** 30 year old, HPAH	Yes Yes
Non PAH - Male	PASMCs	**8.** 72 year old **9.** 76 year old **10.** 62 year old **11.** 54 year old	
PAH - Male	Lung	**i.** 23 year old, HPAH, transplant, meanPAP 54mmHg **j.** 43 year old, IPAH, transplant, meanPAP 62mmHg **k.** 56 year old, IPAH, transplant	Yes

Table E3. Clinical characteristics of the human cells and tissues studied. PASMCs = pulmonary artery smooth muscle cells, IPAH = idiopathic pulmonary hypertension, HPAH = heritable PAH and PAP = pulmonary artery pressure.

References

1. Nelson JF, Felicio LS, Randall PK, Sims C, Finch CE. A longitudinal study of estrous cyclicity in aging c57bl/6j mice: I. Cycle frequency, length and vaginal cytology. *Biol Reprod* 1982;27:327-339.

2. Kasahara Y, Tuder RM, Taraseviciene-Stewart L, Le Cras TD, Abman S, Hirth PK, Waltenberger J, Voelkel NF. Inhibition of vegf receptors causes lung cell apoptosis and emphysema. *J Clin Invest* 2000;106:1311-1319.

3. Abe K, Toba M, Alzoubi A, Ito M, Fagan KA, Cool CD, Voelkel NF, McMurtry IF, Oka M. Formation of plexiform lesions in experimental severe pulmonary arterial hypertension. *Circulation* 2010;121:2747-2754.

4. Ciuclan L, Hussey MJ, Burton V, Good R, Duggan N, Beach S, Jones P, Fox R, Clay I, Bonneau O, Konstantinova L, Pearce A, Rowlands DJ, Jarai G, Westwick J, MacLean MR, Thomas M. Imatinib attenuates hypoxia-induced pulmonary arterial hypertension pathology via reduction in 5-hydroxytryptamine through inhibition of tryptophan hydroxylase 1 expression. *Am J Resp Crit Care* 2013;187:78-89.

5. Keegan A, Morecroft I, Smillie D, Hicks MN, MacLean MR. Contribution of the 5-ht1b receptor to hypoxia-induced pulmonary hypertension - converging evidence using 5-ht1b-receptor knockout mice and the 5-ht1b/1d-receptor antagonist gr127935. *Circ Res* 2001;89:1231-1239.

6. Yang X, Long L, Southwood M, Rudarakanchana N, Upton PD, Jeffery TK, Atkinson C, Chen H, Trembath RC, Morrell NW. Dysfunctional smad signaling contributes to abnormal smooth muscle cell proliferation in familial pulmonary arterial hypertension. *Circ Res* 2005;96:1053-1063.